Electronic Supplementary Material (ESI) for Dalton Transactions.

Supporting Information

Ruthenium Bistridentate Complexes with Non-Symmetrical Hexahydro-pyrimidopyrimidine Ligands: A Structural and Theoretical Investigation of their Optical and Electrochemical Properties.

Baptiste Laramée-Milette and Garry S. Hanan*

* Département de Chimie, Pavillon J.-A. Bombardier, 5155 Chemin de la Rampe, Université de Montréal, Montréal, Québec, Canada, H3T 2B1.

Contents

1. Experimental

Materials and Instrumentations

All solvents and reagents were used as purchased without further purification before the reactions. $RuCl_3.3H_2O$ was purchased from Pressure Chemical Corporation. All other reagents were purchased from Sigma-Aldrich. ACS grade solvents were purchased from VWR and Fisher. Nuclear magnetic resonance (NMR) spectra were recorded in CD_2Cl_2, $CDCl_3$ and CD_3CN at 25°C on a Bruker AV-400 spectrometer at 400 MHz for ^1H NMR and at 100 MHz for ^{13}C NMR. Chemical shifts (δ) are reported in parts per million (ppm) relative to TMS, and are referenced to the residual solvent signal (δ = 1.94 ppm for acetonitrile-d_3, 5.32 ppm for methylene chloride-d_2 and 7.26 ppm for chloroform-d_1). The high-resolution mass spectrometry (HR-MS) experiments were performed on a Bruker Daltonics microTOF spectrometer using electrospray ionization. Absorption and emission spectra were measured in deaerated spectrograde solvent at room temperature on a Cary 300 UV-Vis-NIR Spectrophotometer from Agilent Technologies and a Cary Eclipse Fluorescence Spectrophotometer, respectively. For the luminescence lifetimes, an Edinburgh OB 900 single-photon-counting spectrometer was used, employing a Hamamatsu PLP2 laser diode as pulse (wavelength output, 408 nm; pulse width, 59 ps).

Electrochemical measurements were carried out in argon-purged acetonitrile at room temperature with a BAS CV50W multipurpose potentiostat. The working electrode was a glassy carbon electrode. The counter electrode was a Pt wire, and the pseudo-reference electrode was a silver wire. The reference was set using an internal 1 mM ferrocene/ferrocenium sample at $E_{1/2}$ = 400 mV vs SCE in dry acetonitrile.[1] The concentration of the compounds was of about 1 mM. Tetrabutylammonium hexafluorophosphate (TBAP) was used as the supporting electrolyte and its concentration was 0.10 M. Cyclic voltammograms were obtained at scan rates of 50, 100, 200, and 500 mV/s. For reversible processes, half-wave potentials (vs SCE) were measured with square-wave voltammetry (SW) experiments performed with a step rate of 4 mV, an amplitude of 25 mV and a frequency of 15 Hz. For irreversible reduction processes, the cathodic peak was used as *E*. The criteria for reversibility were the close to unity ratio of the intensities of the cathodic and anodic currents, and the constancy of the peak potential on changing scan rate. Experimental uncertainties are as follows: absorption maxima, ± 2 nm; molar absorption coefficient, 10%; emission maxima, ± 5 nm; excited state lifetimes, 10%; redox potentials, ± 10 mV. The microanalyses were performed at the Elemental Analysis Service of the Université de Montréal.

Synthesis of the ligands and metal complexes

$Ru(DMSO)_4Cl_2$,[2] 6-bromo-2,2'-bipyridine,[3] 2-chloro-1,10-phenanthroline[4] and (4'-phenyl-2,2':6',2"-terpyridine)$RuCl_3$[5] were synthesized as previously described. Solvents were removed under reduced pressure using a rotary evaporator unless otherwise stated.

2,2'-bipyridyl-6-hpp (bpyG, 1)

A 100 mL oven-dried round-bottomed flask was charged with (±)BINAP (16 mg, 3 mol% with respect to 6-bromo-2,2'-bipyridine) under an inert N_2-atmosphere. Dry toluene (10 mL) was added to the flask and the resulting mixture was left at 60°C to give a clear colourless solution. The solution was cooled to room temperature and $Pd(OAc)_2$ catalyst (3.8 mg, 2 mol% with respect to 6-bromo-2,2'-bipyridine) was added to the flask, leading to a clear dark red solution after 5-10 minutes. To this solution was added 6-bromo-2,2'-bipyridine (200 mg, 0.85 mmol) and the mixture was heated at 60°C for 20 minutes, while a color change from red to yellow could be observed. To the resulting solution was added H-hpp (130 mg, 0.94 mmol) and potassium *tert*-butoxide (240 mg, 2.13 mmol) and the resulting brownish-green solution was heated at 90°C for 3 hours. After this time, the reaction mixture was cooled to room temperature and the solvent was evaporated to dryness. The residue was suspended in 25 mL of an ether:toluene (60:10 v/v) mixture and filtered. The filtrate was evaporated to dryness. The residue was subject to a purification over deactivated neutral alumina, using a mixture of methylene chloride and ethanol in a 95:5 ratio, affording a pure white solid (110 mg, 45%).

^1H NMR (400 MHz, CD_2Cl_2): δ (ppm) = 8.64 (d, J = 5 Hz, 1H), 8.15 (m, 2H), 7.97 (t, J = 8 Hz, 1H), 7.82 (t, J = 7 Hz, 1H), 7.48 (d, J = 8 Hz, 1H), 7.32 (d, J = 8 Hz, 1H), 3.97 (t, J = 6 Hz, 2H), 3.62 (m, 4H), 3.50 (t, J=6 Hz, 2H), 2.27 (quint, J = 6 Hz, 2H), 2.07 (quint, J = 6 Hz, 2H). ^{13}C NMR (100 MHz, CD_2Cl_2): δ (ppm) = 153.9, 153.7, 152.5, 150.2, 148.8, 140.3, 136.7, 123.7, 120.6, 118.5, 117.5, 47.7, 47.3, 46.3, 38.2, 20.6, 19.5. HRMS (ESI): m/z $[M+H]^+$ calcd for $C_{17}H_{19}N_5$: 294.17132; found: 294.17265; difference: 4.52 ppm

2-hpp-1,10-phenanthroline (phenG, 2)

Synthesized from 2-chloro-1,10-phenanthroline by following the procedure described above for 1. (825 mg, 87%).

^1H NMR (400 MHz, $CDCl_3$): δ (ppm) = 12.60 (s, 1H), 9.05 (dd, J = 4.3 Hz, 1H), 8.40 (d, J = 8.8 Hz, 1H), 8.26 (dd, J = 8.2 Hz, 1H), 7.94 (d, J = 8.8 Hz, 1H), 7.76 (q, J = 8.8 Hz, 2H), 7.65 (dd, J = 8.1 Hz, 1H), 4.31 (t, J = 6.0 Hz, 2H), 3.80 (t, J = 6.0 Hz, 2H), 3.72 (t, J = 6.0 Hz, 2H), 2.38 (quin, J = 6.0 Hz, 2H), 2.20 (quin, J = 6.0 Hz, 2H), 1.21 (t, J = 7.0, 1H). ^{13}C NMR (100 MHz, $CDCl_3$): δ (ppm) = 153.7, 151.6, 150.6, 144.4, 142.4, 140.5, 136.4, 129.4, 126.6, 125.8, 123.8, 115.8, 49.0, 48.2, 46.9, 39.2, 21.4, 20.1. HRMS (ESI): m/z $[M+H]^+$ calcd for $C_{19}H_{19}N_5$: 318.17132; found: 318.17161; difference: 0.91 ppm

8-(6-bromo-2-pyridinyl)quinolone

A 20 mL microwave vial was charged with 8-quinolinylboronic acid (75 mg, 0.43 mmol), 2,6-dibromopyridine (405 mg, 1.71 mmol), potassium carbonate (340 mg, 2.45 mmol), $Pd_2(dba)_3$ (7.5 mg, 2 mol%), SPhos (6.6 mg, 4 mol%) and 20 mL of a MeCN:H_2O (2:1) solution. The biphasic mixture was degassed for 5 minutes with argon. The mixture was left under microwave heating (400W, 80°C) for 10 minutes. The resulting yellowish solution was extracted 4 times with methylene chloride and the organic layer was evaporated to dryness. The residue was subject to a purification by flash chromatography, using a mixture of hexanes:ethyl acetate (90:10) as the eluent. The fraction containing the desired product were combined and evaporated under reduced pressure, yielding a white solid (25 mg, 20%)

^{1}H NMR (400 MHz, $CDCl_3$): δ (ppm) = 8.95 (dd, J = 2 Hz, 1H), 8.21 (t, J = 8 Hz, 3H), 7.89 (dd, J = 1 Hz, 1H), 7.66 (t, J = 8 Hz, 2H), 7.49 (d, J = 8 Hz, 1H), 7.44 (dd, J = 4 Hz, 1H). ^{13}C NMR (100 MHz, CD_2Cl_2): δ (ppm) = 157.8, 150.3, 145.6, 141.5, 137.8, 136.9, 136.5, 131.6, 129.3, 128.5, 126.5, 126.3, 125.9, 121.1.

2-hpp-6-quinolylpyridine (QpyG, 3)

Synthesized from 8-(6-bromo-2-pyridinyl)quinolone by following the procedure described above for 1. (825 mg, 87%)

^{1}H NMR (400 MHz, CDCl3): δ (ppm) = 8.89 (dd, J = 2 Hz, 1H), 8.27 (dd, J = 2 Hz, 1H), 8.05 (t, J = 8 Hz, 1H), 7.95 (dd, J = 1 Hz, 1H), 7.91 (dd, J = 1 Hz, 1H), 7.66 (t, J = 7 Hz, 1H), 7.62 (d, J = 7 Hz, 1H), 7.55 (d, J = 8 Hz, 1H), 7.48 (dd, J = 4 Hz, 1H), 4.08 (t, J = 6 Hz, 2H), 3.68 (t, J = 6 Hz, 2H), 3.60 (t, J = 6 Hz, 2H), 3.51 (dt, J = 6 Hz, 2H), 2.29 (quint, J = 6 Hz, 2H), 2.11 (quint, J = 6 Hz, 2H). ^{13}C NMR (100 MHz, CD2Cl2): δ (ppm) = 156.1, 153.4, 151.0, 150.7, 145.6, 141.0, 137.2, 136.9, 131.1, 130.0, 129.1, 126.6, 123.2, 121.7, 115.8, 48.5, 48.2, 47.4, 46.9, 21.2, 20.1. HRMS (ESI): m/z $[M+H]^+$ calcd for $C_{21}H_{21}N_5$: 344.18697; found: 344.18649; difference: 1.39 ppm

***mer*-[Ru(bpyG)$_2$][(PF$_6$)$_2$] (4)**

A 20 mL microwave vial was charged with ligand 1 (50 mg, 0.17 mmol), $Ru(DMSO)_4Cl_2$ (40.5 mg, 0.083 mmol), 4-ethylmorpholine (12 drops) and ethylene glycol (15 mL). The vial was then subjected to microwave irradiation (400W, 200°C) for 20 minutes. After this time, the resulting deep purple solution was poured into an aqueous KPF_6 solution (10 eq.). The resulting precipitate was filtered over paper. Recrystallization from slow diffusion of ether into an acetone solution afforded purple needles (40 mg, 50%).

^{1}H NMR (400 MHz, CD_3CN): δ (ppm) = 8.37 (d, J = 8 Hz, 2H), 8.29 (d, J = 8 Hz, 2H), 8.14 (t, J = 8 Hz, 2H), 7.80 (t, J = 8 Hz, 2H), 7.67 (d, J = 5 Hz, 2H), 7.62 (d, J = 8 Hz, 2H), 7.16(t, J = 6 Hz, 2H), 4.04 (dt, J = 4 Hz, 2H), 4.04 (dt, J = 4 Hz, 2H), 3.37-3.30 (m, 4H), 3.14 (dt, J = 9 Hz, 2H), 3.00 (q, J = 6 Hz, 2H), 2.93 (quint, J = 6 Hz, 2H), 2.55 (dq, J = 4 Hz, 2H), 2.38 (m, 2H), 2.15 (m, 2H), 1.83 (dq, J = 4 Hz, 2H), 1.12 (m, 2H). ^{13}C NMR (100 MHz, CD_3CN): δ (ppm) = 158.5, 156.5, 156.1, 153.3, 151.8, 137.0, 135.6, 125.5, 123.9, 119.0, 117.1, 49.9, 49.7, 49.1, 47.8, 30.8, 24.1, 23.7. Calc. for $C_{34}H_{38}N_{10}RuP_2F_{12}\cdot(C_2H_5)_2O$: C, 43.39%; H, 4.60%; N, 13.32%. Found: C, 43.09%; H, 4.45%; N, 13.24%. HRMS (ESI): m/z $[M-PF_6]^+$ calcd for $C_{34}H_{38}N_{10}RuPF_6$: 833.19695; found: 833.19864; difference: 2.03 ppm; $[M-2PF_6]^{2+}$ calcd for $C_{34}H_{38}N_{10}Ru$: 344.11611; found: 344.11664; difference: 1.54 ppm.

***mer*-[Ru(phenG)$_2$][(PF$_6$)$_2$] (5)**

A 20 mL microwave vial was charged with ligand 2 (100 mg, 0.32 mmol), $RuCl_3.3H_2O$ (37 mg, 0.14 mmol), 4-ethylmorpholine (12 drops) and ethylene glycol (15 mL). The vial was then subjected to microwave irradiation (400W, 200°C) for 20 minutes. After this time, the resulting deep purple solution was poured into an aqueous KPF_6 solution (10 eq.). The resulting precipitate was filtered over celite, washed with ethyl acetate and dissolve with a minimum amount of acetonitrile. The solvent were removed under vacuum. Recrystallization from slow diffusion of ether into an acetone solution afforded purple block (85 mg, 52%).

^{1}H NMR (400 MHz, CD_3CN): δ (ppm) = 8.73 (d, J = 9.0 Hz, 2H), 8.34 (d, J = 8.1 Hz, 2H), 8.23 (d, J = 8.8 Hz, 2H), 8.05 (d, J = 8.8 Hz, 2H), 7.97 (m, 4H), 7.45 (dd, J = 8.2 Hz, 2H), 4.30 (dt, J = 5.0 Hz, 2H), 3.60 (m, 2H), 3.42 (m, 2H), 3.14 (m, 2H), 2.95 (m, 2H), 2.81 (m, 2H), 2.71 (m, 2H), 2.46 (m, 2H), 2.22 (m, 2H), 1.84 (m, 2H), 1.31 (m, 2H), 0.78 (m, 2H). ^{13}C NMR (100 MHz, CD_3CN): δ (ppm) = 154.7, 153.6, 151.3, 148.5, 147.2, 135.9, 134.9, 131.0, 127.5, 127.4, 126.9, 124.5, 117.4, 49.6, 49.5, 49.0, 48.7, 24.1, 23.1. Calc. for $C_{38}H_{38}N_{10}RuP_2F_{12}\cdot C_4H_8O_2$: C, 45.29%; H, 4.16%; N, 12.57%. Found: C, 45.36%; H, 4.50%; N, 12.07%. HRMS (ESI): m/z $[M-PF_6]^+$ calcd for $C_{38}H_{38}N_{10}RuPF_6$: 881.19706; found: 881.19717; difference: 0.12 ppm.

***fac*-[Ru(QpyG)$_2$][(PF$_6$)$_2$] (6)**

A 20 mL microwave vial was charged with ligand 3 (50 mg, 0.15 mmol), $RuCl_3.3H_2O$ (19 mg, 0.073 mmol), 4-ethylmorpholine (12 drops) and ethylene glycol (15 mL). The vial was then subjected to microwave irradiation (400W, 200°C) for 20 minutes. After this time, the resulting deep purple solution was poured into an aqueous KPF_6 solution (10 eq.). The resulting precipitate was filtered over paper. The crude mixture was purified over silica using a MeCN:H_2O:NaCl sat. mixture in a 7:2:1 ratio. The major deep purple fraction was then evaporated to dryness and dissolved in a minimum amount of water. The fraction was rechromatographed using SP-Sephadex C25 cation exchanger column (1.5 cm x 35 cm) with 0.15M sodium (-)-*O,O'*-dibenzoyl-L-tartrate solution (pH adjusted between 8 – 9 with NaOH 4M). The major purple band was recovered and a saturated KPF_6 solution (10-15 mL) was added to the fraction. The product was extracted thrice with dichloromethane. The organic layer was then washed with three portions of diluted NaOH 2M in order to remove the remaining excess of (-)-*O,O'*-dibenzoyl-L-tartrate. Recrystallization from slow diffusion of ether into a concentrated acetonitrile solution afforded purple needles (15 mg, 19%).

^{1}H NMR (400 MHz, CD_3CN): δ (ppm) = 9.67 (d, J = 8 Hz, 2H), 8.31 (d, J = 8 Hz, 2H), 7.96 (dd, J = 8 Hz, 4H), 7.61 (dd, J = 8 Hz, 2H), 7.47 (t, J = 8 Hz, 2H), 7.39 (t, J = 8 Hz, 2H), 7.31 (d, J = 8 Hz, 2H), 6.15 (d, J = 8 Hz, 2H), 4.11 (dd, J = 13 Hz, 2H), 3.69 (dt, J = 11 Hz, 2H), 3.50-3.44 (m, 4H), 3.36-3.29 (m, 4H), 3.15-3.08 (m, 6H), 1.84-1.78 (m, 3H), 1.71-1.54 (m, 3H).

^{13}C NMR (100 MHz, CD_3CN): δ (ppm) =160.2, 159.3, 159.0, 151.4, 148.2, 137.8, 137.6, 134.7, 131.4, 130.1, 129.3, 128.3, 123.2, 123.0, 109.8 50.4, 49.4, 48.8, 45.9, 23.8, 22.0. Calc. for $C_{42}H_{42}N_{10}RuP_2F_{12}\cdot 2H_2O$: C, 45.29%; H, 4.16%; N, 12.57%. Found: C, 45.09%; H, 4.01%; N, 12.83%. HRMS (ESI): m/z $[M\text{-}PF_6]^+$ calcd for $C_{42}H_{42}N_{10}RuPF_6$: 933.22847; found: 933.23303; difference: 4.89 ppm; $[M\text{-}2PF_6]^{2+}$ calcd for $C_{42}H_{42}N_{10}Ru$: 394.13187; found: 394.13134; difference: 1.34 ppm.

***mer*-[Ru(bpyG)(phtpy)][(PF_6)$_2$] (7)**

A 20 mL microwave vial was charged with ligand 1 (35 mg, 0.12 mmol), (4'-phenyl-2,2':6',2"-terpyridine)$RuCl_3$ (66.5 mg, 0.129 mmol), 4-ethylmorpholine (12 drops) and ethylene glycol (15 mL). The vial was then subjected to microwave irradiation (400W, 200°C) for 20 minutes. After this time, the resulting orange-red solution was poured into an aqueous KPF_6 solution (10 eq.). The resulting precipitate was filtered over paper. The residue was purified on a silica column with a mixture of MeCN:H_2O:KNO_3 sat. in a 7:2:1 ratio. The isolated species was subjected to a second metathesis with KPF_6 solution (10 eq.). The precipitate was extracted with dichloromethane and the solvent was removed under vacuum. The resulting precipitate was recrystallized by slow diffusion of ether into an acetone solution to afforded orange needles (70 mg, 60%).

^{1}H NMR (400 MHz, CD_3CN): δ (ppm) = 8.84 (s, 2H), 8.56 (d, J = 8 Hz, 2H), 8.42 (d, J = 8 Hz, 1H), 8.35 (d, J = 8 Hz, 1H), 8.31 (t, J = 8 Hz, 1H), 8.15 (d, J = 7 Hz, 2H), 7.97 (t, J = 8 Hz, 2H), 7.79 (d, J = 8 Hz, 1H), 7.75-7.70 (m, 3H), 7.66 (t, J = 7 Hz, 1H), 7.60 (d, J = 5 Hz, 2H), 7.33 (t, J = 7 Hz, 2H), 7.11 (d, J = 5 Hz, 1H), 7.03 (t, J = 7 Hz, 1H), 3.91 (d, J = 6 Hz, 2H), 3.30 (t, J = 7 Hz, 2H), 2.96 (t, J = 6 Hz, 2H), 2.36 (dd, J = 4 Hz, 2H), 2.14 (dd, J = 6 Hz, 2H), 1.23 (dd, J = 6 Hz, 2H). ^{13}C NMR (100 MHz, CD_3CN): δ (ppm) = 159.2, 158.0, 157.8, 155.5, 153.5, 151.9, 147.6, 138.7, 138.3, 137.9, 136.9, 133.1, 131.1, 130.5, 130.3, 128.6, 128.4, 127.2, 124.8, 124.4, 122.3, 119.6, 49.8, 49.7, 48.9, 46.5, 30.8, 24.0, 23.1. Calc. for $C_{38}H_{34}N_8RuP_2F_{12}\cdot C_3H_6O$: C, 46.82%; H, 3.83%; N, 10.65%. Found: C, 46.86%; H, 3.88%; N, 10.60%. HRMS (ESI): m/z $[M\text{-}PF_6]^+$ calcd for $C_{38}H_{34}N_8RuPF_6$: 849.15962; found: 849.15829; difference: 1.57 ppm.

***mer*-[Ru(phenG)(phtpy)][(PF_6)$_2$] (8)**

Synthesized from ligand 2 by following the procedure described above for metal complex 7. (97 mg, 48%).

^{1}H NMR (400 MHz, CD_3CN): δ (ppm) = 8.90 (s, 2H), 8.87 (d, J = 9.1 Hz, 1H), 8.58 (d, J = 7.6 Hz, 2H), 8.30 (t, J = 8.4 Hz, 2H), 8.21 (dd, J = 8.2 Hz, 2H), 8.13 (d, J = 8.1 Hz, 1H), 8.04 (d, J = 8.0 Hz, 1H), 7.92 (dt, J = 8.1 Hz, 2H), 7.74 (tt, J = 7.3 Hz, 2H), 7.68 (tt, J = 7.4 Hz, 1H), 7.53 (m, 2H), 7.47 (dd, J = 5.3 Hz, 1H), 7.36 (dd, J = 8.2 Hz, 1H), 7.20 (m, 2H), 4.11 (t, J = 5.7 Hz, 2H), 3.37 (t, J = 7.4 Hz, 2H), 3.04 (t, J = 6.2 Hz, 2H), 2.46 (m, 2H), 2.32 (t, J = 5.7 Hz, 2H), 1.30 (m, 2H). ^{13}C NMR (100 MHz, CD_3CN): δ (ppm) = 161.0, 159.4, 158.2, 154.4, 153.7, 152.9, 152.3, 147.7, 147.5, 146.2, 138.3, 138.1, 137.8, 136.3, 131.3, 131.1, 130.6, 128.7, 128.4, 1128.3, 128.0, 127.0, 125.5, 124.9, 122.3, 49.8, 49.5, 49.2, 47.7, 24.2, 23.1. Calc. for $C_{40}H_{34}N_8RuP_2F_{12}\cdot(C_2H_5)_2O$: C, 48.40%; H, 4.06%; N, 10.26%. Found: C, 47.97%; H, 3.92%; N, 10.20%. HRMS (ESI): m/z $[M\text{-}PF_6]^+$ calcd for $C_{40}H_{34}N_8RuPF_6$: 873.15968; found: 873.16233; difference: 3.03 ppm.

***mer*-[Ru(QpyG)(phtpy)][(PF_6)$_3$] (9)**

Synthesized from ligand 3 by following the procedure described above for metal complex 7. (14.5 mg, 10%).

^{1}H NMR (400 MHz, CD_3CN): δ (ppm) = 8.70-60 (m, broad), 8.55-8.47 (m, broad), 8.43 (d, broad), 8.30-8.19 (m, broad), 8.16-8.04 (m, broad), 8.01 (d, broad), 7.96-7.90 (m, broad), 7.88-7.83 (m, broad), 7.77 (d, broad), 7.72-7.66 (m, broad), 7.65-7.57 (m, broad), 3.27-3.14 (m, broad), 2.91-2.83 (m, broad), 2.41-2.25 (m, broad), 1.82-1.72 (m, broad), 1.33-1.25 (m, broad), 1.20-1.10 (m, broad). ^{13}C NMR (100 MHz, CD_3CN): δ (ppm) = No peak was observed due to the paramagnetic nature of the compound. HRMS (ESI): m/z $[M\text{-}PF_6]^+$ calcd for $C_{42}H_{36}N_8RuPF_6$: 899.17538; found: 899.17326; difference: 2.36 ppm

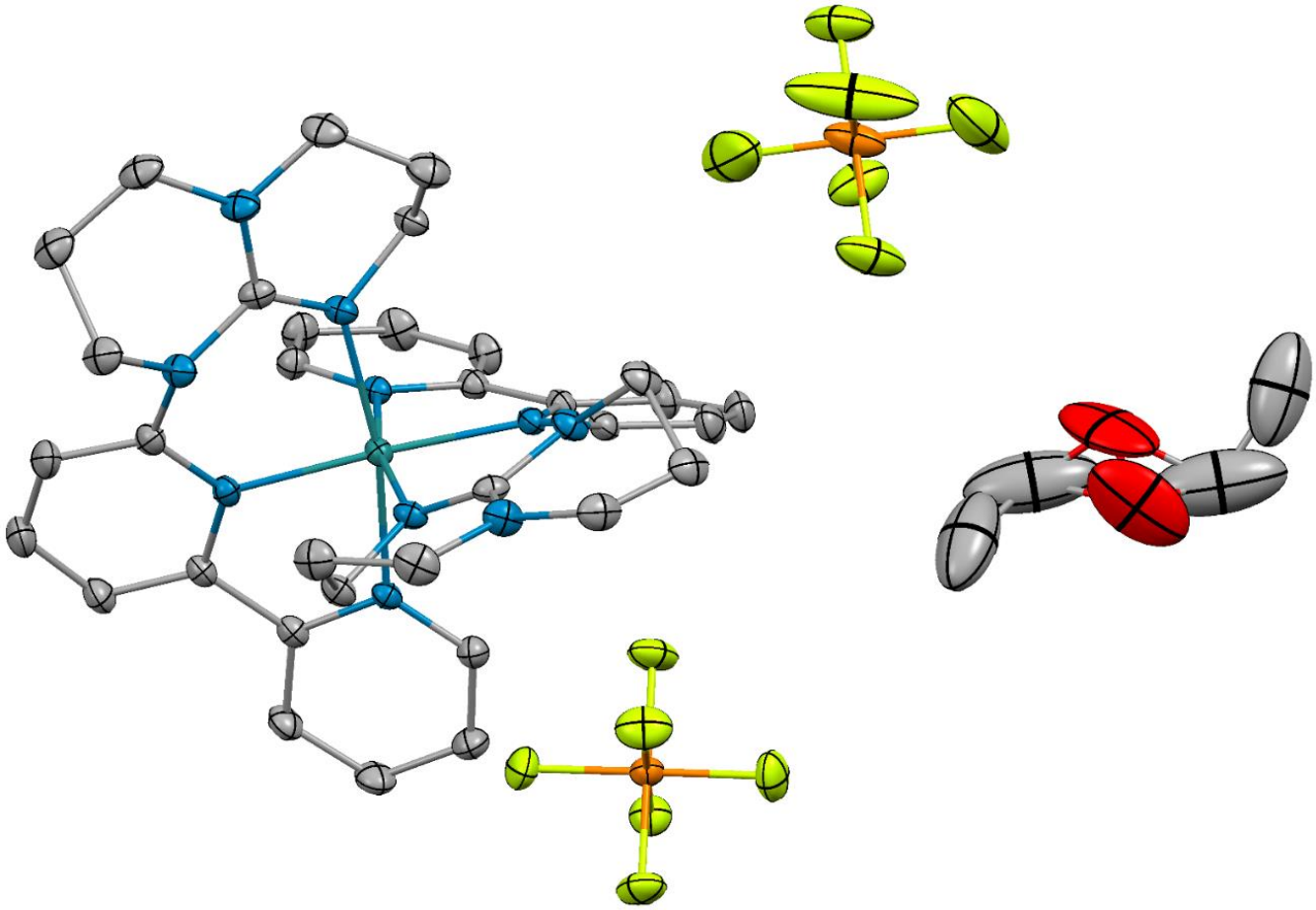

Figure S1 – Thermal ellipsoid diagram (30% probability) of the single crystal of **4** with the counter-anions (PF_6) and a disordered diethyl ether co-crystallization solvent molecule. The hydrogens atoms are omitted for clarity.

Table 2 – Atomic coordinates for DFT optimization of $\mathbf{4}^{2+}$ in (*S* = 0) PBE0/LANL2DZ, CPCM(CH_3CN).

Standard orientation					
Center Number	Atomic Number	Atomic Type	Coordinates (Angstroms)		
			X	Y	Z
1	44	0	-0.000219	0.479713	0.000006
2	7	0	1.824154	0.623289	0.881213
3	7	0	-0.370106	1.980844	1.368745
4	7	0	0.732269	-0.946179	-1.330792
5	7	0	2.202619	-2.710516	-1.909561
6	7	0	2.622483	-1.465294	0.031346
7	6	0	1.999801	1.734069	1.674596
8	6	0	2.855581	-0.235586	0.671366
9	6	0	0.763061	2.475503	1.966180
10	6	0	-1.566647	2.552917	1.647821
11	1	0	-2.434813	2.121020	1.167853
12	6	0	1.808133	-1.674940	-1.096102
13	6	0	3.248772	2.061351	2.203444
14	1	0	3.381175	2.940160	2.820592
15	6	0	3.555970	-3.305096	-1.955585

16	1	0	4.028198	-3.039252	-2.910380
17	1	0	3.420044	-4.393939	-1.950455
18	6	0	-1.689282	3.643334	2.510613
19	1	0	-2.667983	4.066763	2.703077
20	6	0	0.090745	-1.166319	-2.643524
21	1	0	0.710671	-0.728541	-3.440544
22	1	0	-0.868072	-0.653469	-2.652103
23	6	0	-0.534752	4.168995	3.108832
24	1	0	-0.595120	5.019389	3.778617
25	6	0	0.700533	3.573166	2.835155
26	1	0	1.599045	3.957228	3.301747
27	6	0	1.301793	-3.296669	-2.923002
28	1	0	1.247031	-4.379027	-2.748427
29	1	0	1.758323	-3.146425	-3.910710
30	6	0	3.490233	-2.610703	0.393615
31	1	0	2.847993	-3.479191	0.581858
32	1	0	4.011831	-2.388504	1.323466
33	6	0	4.430302	-2.894267	-0.770761
34	1	0	5.018274	-1.999214	-1.000381
35	1	0	5.129725	-3.700083	-0.530339
36	6	0	4.143861	0.076520	1.155301
37	1	0	4.986336	-0.561335	0.923594
38	6	0	-0.082809	-2.664326	-2.884267
39	1	0	-0.686609	-3.090466	-2.075204
40	1	0	-0.600744	-2.858007	-3.828805
41	6	0	4.338198	1.231160	1.912020
42	1	0	5.329263	1.479792	2.274371
43	7	0	-1.824717	0.621765	-0.881189
44	7	0	0.368411	1.981126	-1.368770
45	7	0	-0.731519	-0.946756	1.330818
46	7	0	-2.200255	-2.712447	1.909516
47	7	0	-2.621271	-1.467504	-0.031331
48	6	0	-2.001300	1.732405	-1.674557
49	6	0	-2.855426	-0.237967	-0.671316
50	6	0	-0.765174	2.474848	-1.966186
51	6	0	1.564475	2.554174	-1.647882
52	1	0	2.433008	2.122999	-1.167928
53	6	0	-1.806725	-1.676477	1.096097
54	6	0	-3.250557	2.058679	-2.203348
55	1	0	-3.383699	2.937380	-2.820491
56	6	0	-3.553043	-3.308305	1.955500
57	1	0	-4.025495	-3.043038	2.910345
58	1	0	-3.416101	-4.397021	1.950209
59	6	0	1.686197	3.644677	-2.510697
60	1	0	2.664547	4.068904	-2.703189

61	6	0	-0.089836	-1.166348	2.643562
62	1	0	-0.710217	-0.729210	3.440579
63	1	0	0.868488	-0.652577	2.652208
64	6	0	0.531223	4.169381	-3.108899
65	1	0	0.590879	5.019810	-3.778703
66	6	0	-0.703567	3.572545	-2.835180
67	1	0	-1.602405	3.955858	-3.301762
68	6	0	-1.298852	-3.297883	2.922863
69	1	0	-1.243041	-4.380160	2.748121
70	1	0	-1.755530	-3.148230	3.910592
71	6	0	-3.487996	-2.613684	-0.393631
72	1	0	-2.844978	-3.481590	-0.581908
73	1	0	-4.009805	-2.391941	-1.323469
74	6	0	-4.427782	-2.898136	0.770756
75	1	0	-5.016511	-2.003602	1.000464
76	1	0	-5.126521	-3.704537	0.530309
77	6	0	-4.143992	0.073133	-1.155147
78	1	0	-4.985955	-0.565367	-0.923357
79	6	0	0.085147	-2.664201	2.884225
80	1	0	0.689391	-3.089708	2.075163
81	1	0	0.603226	-2.857447	3.828774
82	6	0	-4.339301	1.227623	-1.911846
83	1	0	-5.330589	1.475476	-2.274119

Table 3 - Selected bond distances and angles of **4**

Bond Length			**Angle**		
	Obs. (X-ray)	**Calc. (DFT)**		**Obs. (X-ray)**	**Calcl. (DFT)**
N1-Ru1 **N1'-Ru1**	2.0542 (17)	2.06487	**N1-Ru1-N1'**	86.59 (9)	86.720
			N1-Ru1-N2	79.63 (7)	79.742
			N1-Ru1-N2'	94.03 (7)	94.350
			N1-Ru1-N4	169.27 (7)	169.715
N2-Ru1 **N2'-Ru1**	2.0165 (18)	2.03113	**N1-Ru1-N4'**	91.98 (7)	90.656
			N2-Ru1-N1'	94.03 (7)	94.349
			N2-Ru1-N2'	171.35 (10)	171.936
			N2-Ru1-N4	89.88 (7)	90.556
N4-Ru1 **N4'-Ru1**	2.0621 (18)	2.08343	**N2-Ru1-N4'**	96.16 (7)	94.965
			N4-Ru1-N1'	91.98 (7)	90.656
			N4-Ru1-N2'	96.17 (7)	94.965
			N4-Ru1-N4'	91.36 (10)	93.602

Table 4. Total energy values for the optimized structure of the first and second oxidation on complex **4** (uPBE1PBE, LANL2DZ, CPCM: Acetonitrile).

4	S	2S+1	Total Energy			Experimental
			a. u.	eV	ΔeV	eV
Neutral	0	1	-1957.34027912	-53261.96169984	-	-
1st oxidation	1/2	2	-1957.17249935	-53257.39617805	4.57	4.68
2nd oxidation	1	3	-1956.92448050	-53250.67723888	6.72	5.87

Table 5. Spin contamination monitoring for the DFT calculation of **4** oxidized species.

4	S	2S+1	S**2		
			Before annihilation	After annihilation	% change
1st oxidation	1/2	2	0.7549	0.7500	1
2nd oxidation	1	3	2.0162	2.0002	1

Table 6. Mulliken spin density values for each of the oxidized **4** species.

4	Mulliken spin density		
	Ruthenium	2,2'-bpy	hpp
1st oxidation	0.782 (78%)	-0.008 (0%)	0.228 (23%)
2nd oxidation	0.764 (38%)	0.013 (1%)	1.318 (66%)

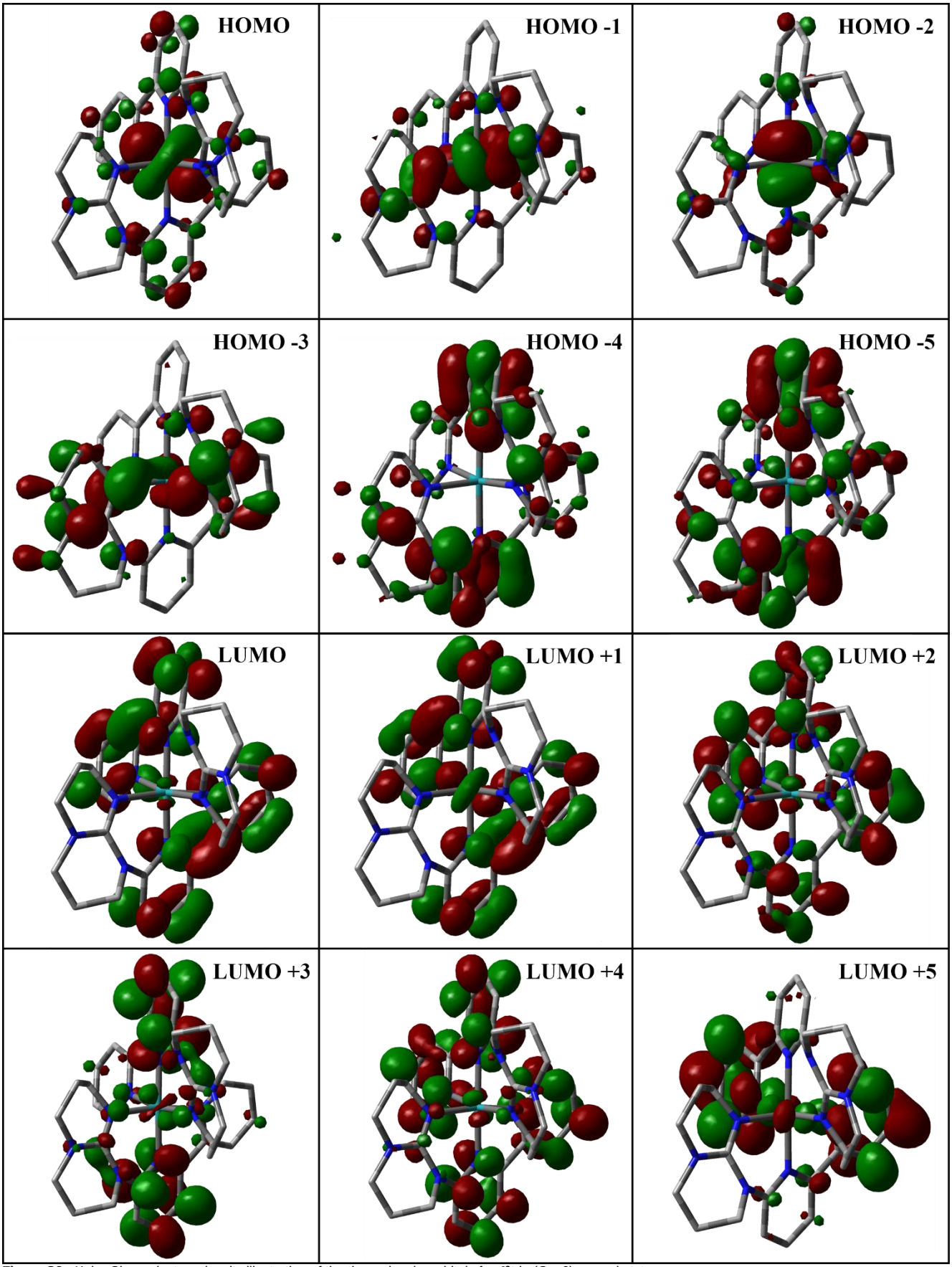

Figure S2 - Kohn-Sham electron density illustration of the the molecular orbitals for $\mathbf{4}^{2+}$ in (S = 0) ground state.

Table S7. MO composition of **4^{2+}** in (*S=0*) ground state.

MO	Energy (eV)	Composition		
		Ruthenium	bpyG	
			2,2'-bipyridyl	hpp
LUMO+5	-0.125	1	92	6
LUMO+4	-1.348	5	94	1
LUMO+3	-1.389	2	88	9
LUMO+2	-1.551	2	94	4
LUMO+1	-2.295	9	90	1
LUMO	**-2.589**	**1**	**98**	**1**
HOMO	**-5.259**	**59**	**29**	**9**
HOMO-1	-6.073	69	24	7
HOMO-2	-6.173	78	12	9
HOMO-3	-6.752	4	6	79
HOMO-4	-7.126	0	51	44
HOMO-5	-7.175	5	54	37

Table S8 - Selected transitions from TD-DFT calculations of **4^{2+}** in the singlet ground state (PBE0), CPCM (CH_3CN).

Energy (eV)	**λ (nm)**	**f**	**Transition**	**Character**
1.69	735	0.0064	H→L (99%)	hpp to bpy ; Ru to bpy
1.84	674	0.0070	H→L+1 (97%)	hpp to bpy ; Ru to bpy
2.53	491	0.0671	H-2→L+1 (17%) H-1→L (79%)	Ru to bpy
2.66	466	0.0617	H-2→L+1 (77%) H-1→L (16%)	Ru to bpy
2.97	418	0.0456	H→L+4 (87%)	hpp to bpy ; Ru to bpy
3.17	391	0.0891	H-1→L+1 (30%) H→L+5 (52%)	hpp to bpy ; Ru to bpy
3.88	320	0.1271	H-4→L (68%) H-1→L+5 (17%)	hpp to bpy ; Ru to bpy
3.93	316	0.2899	H-5→L (70%) H-1→L+4 (15%)	hpp to bpy ; Ru to bpy
4.76	261	0.1792	H-7→L (55%) H-4→L+2 (22%)	hpp to bpy
4.84	256	0.1748	H-8→L (11%) H-2→L+13 (11%) H-1→L+10 (14%) H→L+8 (33%)	Ru to bpy
4.91	252	0.1307	H-8→L (57%) H-5→L+2 (15%)	hpp to bpy ; Ru to bpy
5.05	246	0.1337	H-7→L+1 (81%)	hpp to bpy
5.21	238	0.1147	H-6→L+2 (67%)	hpp to bpy ; Ru to bpy
5.76	215	0.1089	H-12→L (23%) H-10→L+1 (16%) H-7→L+2 (31%)	hpp to bpy

Table S9 – Atomic coordinates for DFT optimization of $\mathbf{5}^{2+}$ in (S = 0) PBE0/LANL2DZ, CPCM(CH_3CN).

Standard orientation					
Center Number	Atomic Number	Atomic Type	Coordinates (Angstroms)		
			X	Y	Z
1	6	0	4.191292	-1.082350	0.240532
2	6	0	4.804589	-0.032138	-0.418386
3	7	0	2.015209	-0.204226	-0.245035
4	6	0	4.018412	0.946975	-1.074387
5	6	0	2.768678	-1.178829	0.306427
6	6	0	2.621094	0.814674	-0.952485
7	6	0	4.554143	2.031224	-1.850277
8	6	0	3.722542	2.906120	-2.504708
9	6	0	2.293287	2.758382	-2.433076
10	6	0	1.383366	3.592520	-3.129534
11	6	0	1.753766	1.717125	-1.638711
12	6	0	0.019054	3.346784	-3.018575
13	6	0	-0.441392	2.288469	-2.209091
14	7	0	0.397909	1.492271	-1.522812
15	7	0	2.173594	-2.323440	0.884214
16	6	0	2.370252	-4.788521	1.355119
17	7	0	0.696402	-3.402798	2.395472
18	6	0	1.741568	-4.395031	2.682630
19	6	0	0.915968	-2.360064	1.529936
20	6	0	3.046686	-3.540781	0.817460
21	7	0	0.000000	-1.418016	1.356200
22	6	0	-1.733222	-2.830319	2.363815
23	6	0	-0.660498	-3.799129	2.846000
24	6	0	-1.108007	-1.438450	2.330228
25	44	0	0.000000	0.000000	-0.159238
26	6	0	-4.191292	1.082350	0.240532
27	6	0	-4.804589	0.032138	-0.418386
28	7	0	-2.015209	0.204226	-0.245035
29	6	0	-4.018412	-0.946975	-1.074387
30	6	0	-2.768678	1.178829	0.306427
31	6	0	-2.621094	-0.814674	-0.952485
32	6	0	-4.554143	-2.031224	-1.850277
33	6	0	-3.722542	-2.906120	-2.504708
34	6	0	-2.293287	-2.758382	-2.433076
35	6	0	-1.383366	-3.592520	-3.129534
36	6	0	-1.753766	-1.717125	-1.638711
37	6	0	-0.019054	-3.346784	-3.018575
38	6	0	0.441392	-2.288469	-2.209091
39	7	0	-0.397909	-1.492271	-1.522812
40	7	0	-2.173594	2.323440	0.884214
41	6	0	-2.370252	4.788521	1.355119

42	7	0	-0.696402	3.402798	2.395472
43	6	0	-1.741568	4.395031	2.682630
44	6	0	-0.915968	2.360064	1.529936
45	6	0	-3.046686	3.540781	0.817460
46	7	0	0.000000	1.418016	1.356200
47	6	0	1.733222	2.830319	2.363815
48	6	0	0.660498	3.799129	2.846000
49	6	0	1.108007	1.438450	2.330228
50	1	0	-1.598682	5.166934	0.675873
51	1	0	-3.128707	5.567051	1.479149
52	1	0	-4.812243	1.820563	0.725370
53	1	0	-3.364484	3.669858	-0.221796
54	1	0	-5.887444	-0.033048	-0.441543
55	1	0	-5.632456	-2.137898	-1.919756
56	1	0	-4.131709	-3.717504	-3.098862
57	1	0	-1.755436	-4.404517	-3.746056
58	1	0	0.704963	-3.957838	-3.544710
59	1	0	1.499312	-2.079442	-2.116493
60	1	0	-3.935633	3.372322	1.432446
61	1	0	-2.495053	3.983333	3.366214
62	1	0	-1.270568	5.244623	3.180060
63	1	0	0.860385	4.815741	2.483539
64	1	0	0.642489	3.835170	3.941620
65	1	0	2.594654	2.867904	3.037848
66	1	0	2.080134	3.093068	1.358431
67	1	0	0.726495	1.179899	3.329943
68	1	0	1.830667	0.677071	2.048188
69	1	0	-1.830667	-0.677071	2.048188
70	1	0	-0.726495	-1.179899	3.329943
71	1	0	-2.594654	-2.867904	3.037848
72	1	0	-2.080134	-3.093068	1.358431
73	1	0	-0.860385	-4.815741	2.483539
74	1	0	-0.642489	-3.835170	3.941620
75	1	0	1.270568	-5.244623	3.180060
76	1	0	2.495053	-3.983333	3.366214
77	1	0	1.598682	-5.166934	0.675873
78	1	0	3.128707	-5.567051	1.479149
79	1	0	3.935633	-3.372322	1.432446
80	1	0	3.364484	-3.669858	-0.221796
81	1	0	4.812243	-1.820563	0.725370
82	1	0	5.887444	0.033048	-0.441543
83	1	0	5.632456	2.137898	-1.919756
84	1	0	4.131709	3.717504	-3.098862
85	1	0	1.755436	4.404517	-3.746056
86	1	0	-0.704963	3.957838	-3.544710

87	1	0	-1.499312	2.079442	-2.116493

Table S10. Total energy values for the optimized structure of the first and second oxidation on complex **5** (uPBE1PBE, LANL2DZ, CPCM: Acetonitrile).

5	S	2S+1	Total Energy			Experimental
			a. u.	eV	ΔeV	eV
Neutral	0	1	-2109.61215483	-57405.498080329	-	-
1st oxidation	1/2	2	-2109.42863809	-57400.504333094	4.99	4.68
2nd oxidation	1	3	-2109.20775581	-57394.493817241	6.01	5.80

TableS11. Spin contamination monitoring for the DFT calculation of **5** oxidized species.

5	S	2S+1	S**2		
			Before annihilation	After annihilation	% change
1st oxidation	1/2	2	0.7576	0.7500	1
2nd oxidation	1	3	2.0157	2.0001	1

Table S12. Mulliken spin density values for each of the oxidized **5** species.

5	Mulliken spin density		
	Ruthenium	1,10-phenanthroline	hpp
1st oxidation	0.879 (88%)	-0.004 (0%)	0.126 (13%)
2nd oxidation	0.979 (49%)	0.015 (1%)	1.006 (50%)

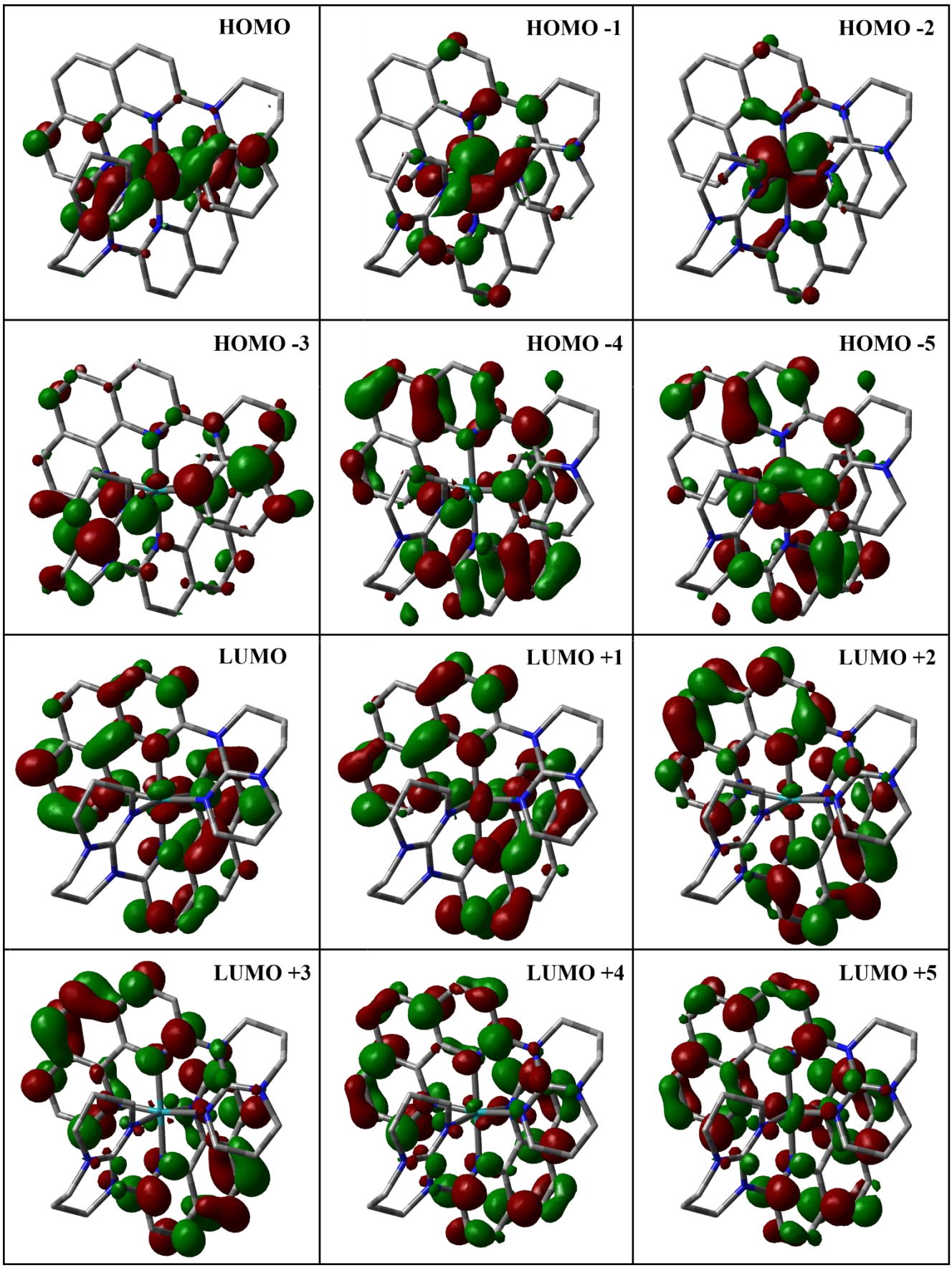

Figure S3 - Kohn-Sham electron density illustration of the the molecular orbitals for $\mathbf{5}^{2+}$ in (S = 0) ground state

Table S13. MO composition of $\mathbf{5^{2+}}$ in (*S=0*) ground state.

MO	Energy (eV)	Composition		
		Ruthenium	phenG	
			1,10-phenanthroline	hpp
LUMO+5	-0.848	4	83	13
LUMO+4	-0.923	4	81	15
LUMO+3	-2.185	2	97	1
LUMO+2	-2.206	2	95	3
LUMO+1	-2.302	4	92	4
LUMO	**-2.322**	**2**	**92**	**6**
HOMO	**-5.362**	**58**	**8**	**33**
HOMO-1	-5.443	63	14	23
HOMO-2	-6.021	86	9	6
HOMO-3	-6.706	8	9	83
HOMO-4	-6.948	7	55	38
HOMO-5	-7.078	9	57	34

Table S14 - Selected transitions from TD-DFT calculations of $\mathbf{5^{2+}}$ in the singlet ground state (PBE0), CPCM (CH_3CN).

Energy (eV)	λ (nm)	f	Transition	Character
2,32	533	0,1311	H-1→L+1 (74%) HOMO→LUMO (21%)	Ru to phen; hpp to phen
4,01	309	0,0942	H-4→L+3 (11%) H-3→LUMO (10%) H-3→L+2 (69%)	hpp to phen
4,04	307	0,2253	H-4→L+2 (29%) H-3→L+3 (49%)	hpp to phen
4,37	283	0,0863	HOMO→L+7 (75%)	Ru to phen; hpp to phen
4,47	278	0,0907	H-1→L+6 (60%) HOMO→L+7 (11%)	Ru to phen; hpp to phen
4,55	273	0,2552	H-8→L+1 (13%) H-7→LUMO (49%)	hpp to phen
4,59	270	0,1672	H-1→L+7 (37%) HOMO→L+6 (20%)	Ru to phen; hpp to phen
4,74	262	0,2009	H-8→L+1 (14%) H-8→L+3 (12%) H-7→L+2 (39%)	Ru to phen; hpp to phen
5,02	247	0,1802	H-1→L+8 (16%) HOMO→L+9 (38%) HOMO→L+10 (14%)	Ru to phen; Ru to hpp
5,16	240	0,1464	H-9→L+1 (56%) H-4→L+4 (13%)	hpp to phen
5,31	233	0,1793	H-10→LUMO (27%) H-9→L+1 (27%) H-9→L+3 (13%) H-3→L+5 (13%)	hpp to phen
5,38	230	0,1556	H-10→LUMO (10%) H-9→L+3 (68%)	hpp to phen
5,44	228	0,4247	H-10→LUMO (29%) H-4→L+4 (47%)	hpp to phen
5,55	224	0,1228	H-10→L+2 (56%) H-5→L+5 (17%)	hpp to phen
5,58	222	0,0769	H-12→LUMO (15%) H-11→L+1 (35%) H-5→L+5 (22%)	hpp to phen
5,60	222	0,1420	H-12→LUMO (14%) H-11→L+1 (12%) H-2→L+9 (25%) H-2→L+10 (11%)	Ru to phen; hpp to phen
5,61	221	0,1716	H-10→L+2 (26%) H-6→L+4 (16%) H-5→L+5 (16%)	Ru to phen; hpp to phen
5,71	217	0,1114	H-12→L (32%) H-11→L+1 (35%)	hpp to phen
593	209	0,0981	H-1→L+13 (22%) H-1→L+15 (60%)	Ru to phen; hpp to phen

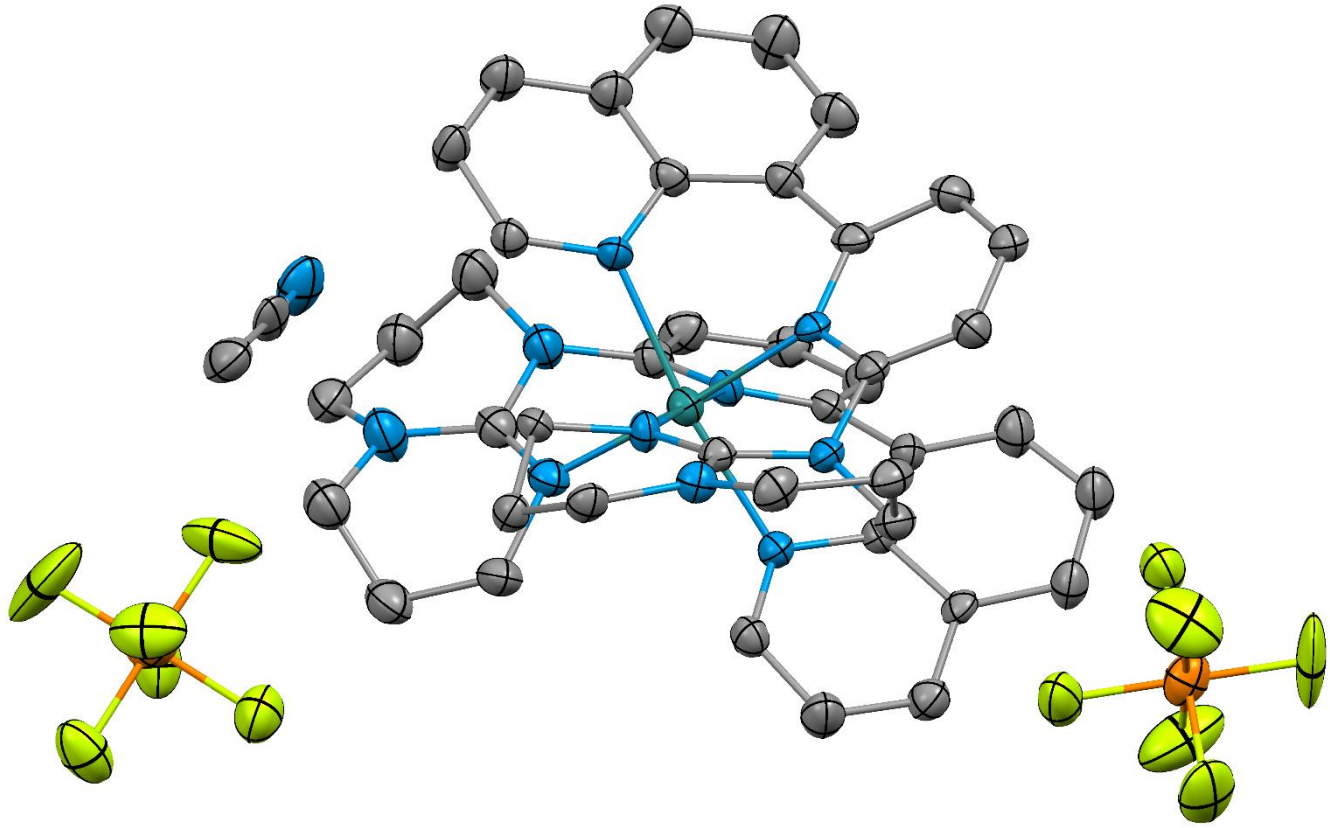

Figure S4 – Thermal ellipsoid diagram (30% probability) of the single crystal of $\mathbf{6}^{2+}$ with the counter-anions (PF_6) and an acetonitrile solvent molecule. The hydrogens atoms are omitted for clarity.

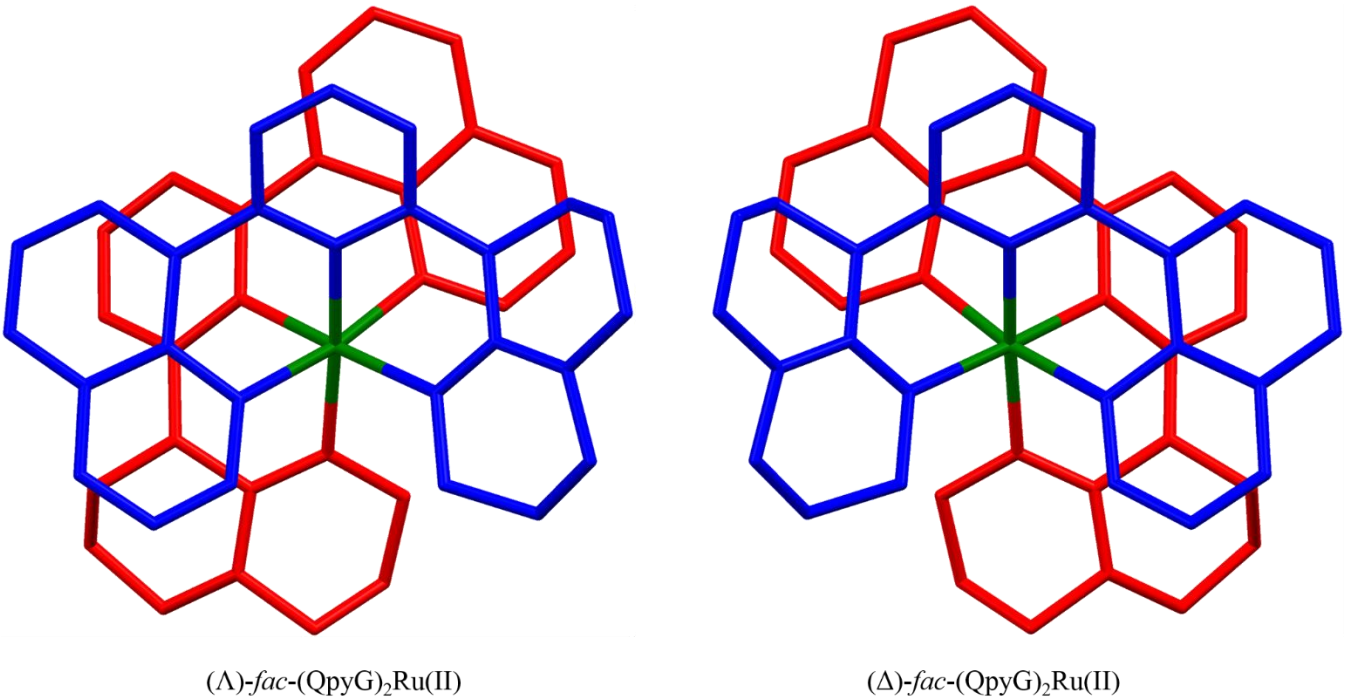

Figure S5 – Capped stick view of both delta and lambda enantiomers found in the unit cell of metal complex $\mathbf{6}^{2+}$. The hydrogens atoms, the counter-anions (PF_6) and the solvent molecule (acetonitrile) are omitted for clarity.

Table S15 – Atomic coordinates for DFT optimization of $\mathbf{6}^{2+}$ in (S = 0) PBE0/LANL2DZ, CPCM(CH_3CN).

Standard orientation					
Center Number	Atomic Number	Atomic Type	Coordinates (Angstroms)		
			X	Y	Z
1	6	0	0.426807	2.472986	-3.443585
2	6	0	0.103038	4.060480	-1.169455
3	6	0	0.705446	1.898296	-2.200980
4	6	0	-0.009757	3.810972	-3.579900
5	6	0	-0.098554	4.618467	-2.462187
6	6	0	0.389181	2.662016	-1.025896
7	6	0	1.531297	0.665515	-2.161308
8	6	0	3.394571	-1.381815	-2.000737
9	6	0	2.429041	0.446574	-3.219510
10	7	0	1.513365	-0.174220	-1.074845
11	6	0	2.482279	-1.132636	-0.960940
12	6	0	3.339395	-0.607987	-3.155932
13	7	0	2.568805	-1.886208	0.223273
14	6	0	4.629646	-3.060381	0.811601
15	6	0	4.445928	-2.649908	2.273800
16	6	0	3.235797	-3.206099	0.206122
17	6	0	2.447853	-1.297260	1.489987
18	7	0	3.217716	-1.852653	2.475163
19	7	0	1.578762	-0.323490	1.709640
20	6	0	1.766092	0.546328	2.895764
21	6	0	2.857353	0.092808	3.872890
22	6	0	2.925692	-1.430938	3.851801
23	1	0	-0.344314	5.672713	-2.547857
24	1	0	-0.217799	4.206233	-4.568316
25	1	0	0.573168	1.888921	-4.345831
26	1	0	2.457942	1.127352	-4.058808
27	1	0	4.040373	-0.781125	-3.964833
28	1	0	4.164280	-2.133325	-1.894953
29	1	0	3.245219	-3.595370	-0.811059
30	1	0	2.638998	-3.897309	0.809783
31	1	0	4.352896	-3.543298	2.902533
32	1	0	5.310614	-2.078305	2.634704
33	1	0	5.183335	-4.002363	0.760700
34	1	0	5.201051	-2.306959	0.258571
35	1	0	3.714873	-1.811111	4.503478
36	1	0	1.973007	-1.866923	4.181055
37	1	0	2.632980	0.466581	4.876934
38	1	0	3.835080	0.492029	3.579067
39	1	0	0.805244	0.615422	3.415526
40	1	0	2.014510	1.549929	2.536112
41	6	0	0.000000	4.862933	-0.000278

42	6	0	0.093760	4.263774	1.240364
43	6	0	0.197784	2.858984	1.306862
44	7	0	0.328858	2.069466	0.227951
45	1	0	-0.172903	5.930015	-0.100168
46	1	0	0.022180	4.833231	2.159179
47	1	0	0.105735	2.360268	2.259260
48	44	0	0.000000	0.000000	0.321625
49	6	0	-0.426807	-2.472986	-3.443585
50	6	0	-0.103038	-4.060480	-1.169455
51	6	0	-0.705446	-1.898296	-2.200980
52	6	0	0.009757	-3.810972	-3.579900
53	6	0	0.098554	-4.618467	-2.462187
54	6	0	-0.389181	-2.662016	-1.025896
55	6	0	-1.531297	-0.665515	-2.161308
56	6	0	-3.394571	1.381815	-2.000737
57	6	0	-2.429041	-0.446574	-3.219510
58	7	0	-1.513365	0.174220	-1.074845
59	6	0	-2.482279	1.132636	-0.960940
60	6	0	-3.339395	0.607987	-3.155932
61	7	0	-2.568805	1.886208	0.223273
62	6	0	-4.629646	3.060381	0.811601
63	6	0	-4.445928	2.649908	2.273800
64	6	0	-3.235797	3.206099	0.206122
65	6	0	-2.447853	1.297260	1.489987
66	7	0	-3.217716	1.852653	2.475163
67	7	0	-1.578762	0.323490	1.709640
68	6	0	-1.766092	-0.546328	2.895764
69	6	0	-2.857353	-0.092808	3.872890
70	6	0	-2.925692	1.430938	3.851801
71	1	0	0.344314	-5.672713	-2.547857
72	1	0	0.217799	-4.206233	-4.568316
73	1	0	-0.573168	-1.888921	-4.345831
74	1	0	-2.457942	-1.127352	-4.058808
75	1	0	-4.040373	0.781125	-3.964833
76	1	0	-4.164280	2.133325	-1.894953
77	1	0	-3.245219	3.595370	-0.811059
78	1	0	-2.638998	3.897309	0.809783
79	1	0	-4.352896	3.543298	2.902533
80	1	0	-5.310614	2.078305	2.634704
81	1	0	-5.183335	4.002363	0.760700
82	1	0	-5.201051	2.306959	0.258571
83	1	0	-3.714873	1.811111	4.503478
84	1	0	-1.973007	1.866923	4.181055
85	1	0	-2.632980	-0.466581	4.876934
86	1	0	-3.835080	-0.492029	3.579067

87	1	0	-0.805244	-0.615422	3.415526
88	1	0	-2.014510	-1.549929	2.536112
89	6	0	0.000000	-4.862933	-0.000278
90	6	0	-0.093760	-4.263774	1.240364
91	6	0	-0.197784	-2.858984	1.306862
92	7	0	-0.328858	-2.069466	0.227951
93	1	0	0.172903	-5.930015	-0.100168
94	1	0	-0.022180	-4.833231	2.159179
95	1	0	-0.105735	-2.360268	2.259260

Table S16 - Selected bond distances and angles of **6**

Bond Length			**Angle**		
	Obs. (X-ray)	**Calc. (DFT)**		**Obs. (X-ray)**	**Calcl. (DFT)**
N1-Ru1	2.085 (3)	2.09753	**N1-Ru1-N2**	85.84 (13)	86.456
			N1-Ru1-N5	95.29 (14)	93.602
N2-Ru1	2.056 (3)	2.06658	**N1-Ru1-N6**	172.21 (12)	174.881
			N1-Ru1-N7	88.93 (13)	90.084
N5-Ru1	2.091 (3)	2.12690	**N1-Ru1-N10**	91.52 (12)	89.740
			N2-Ru1-N5	82.93 (13)	83.373
N6-Ru1	2.097 (3)	2.09753	**N2-Ru1-N6**	89.24 (13)	90.084
			N2-Ru1-N7	96.75 (12)	94.977
N7-Ru1	2.035 (3)	2.06658	**N2-Ru1-N10**	177.26 (13)	175.855
			N5-Ru1-N6	90.09 (14)	89.740
N10-Ru1	2.094 (3)	2.12690	**N5-Ru1-N7**	175.73 (14)	175.855
			N5-Ru1-N10	96.62 (12)	98.524
			N6-Ru1-N7	85.65 (13)	86.456
			N6-Ru1-N10	93.46 (12)	93.602
			N7-Ru1-N10	83.90 (12)	83.373

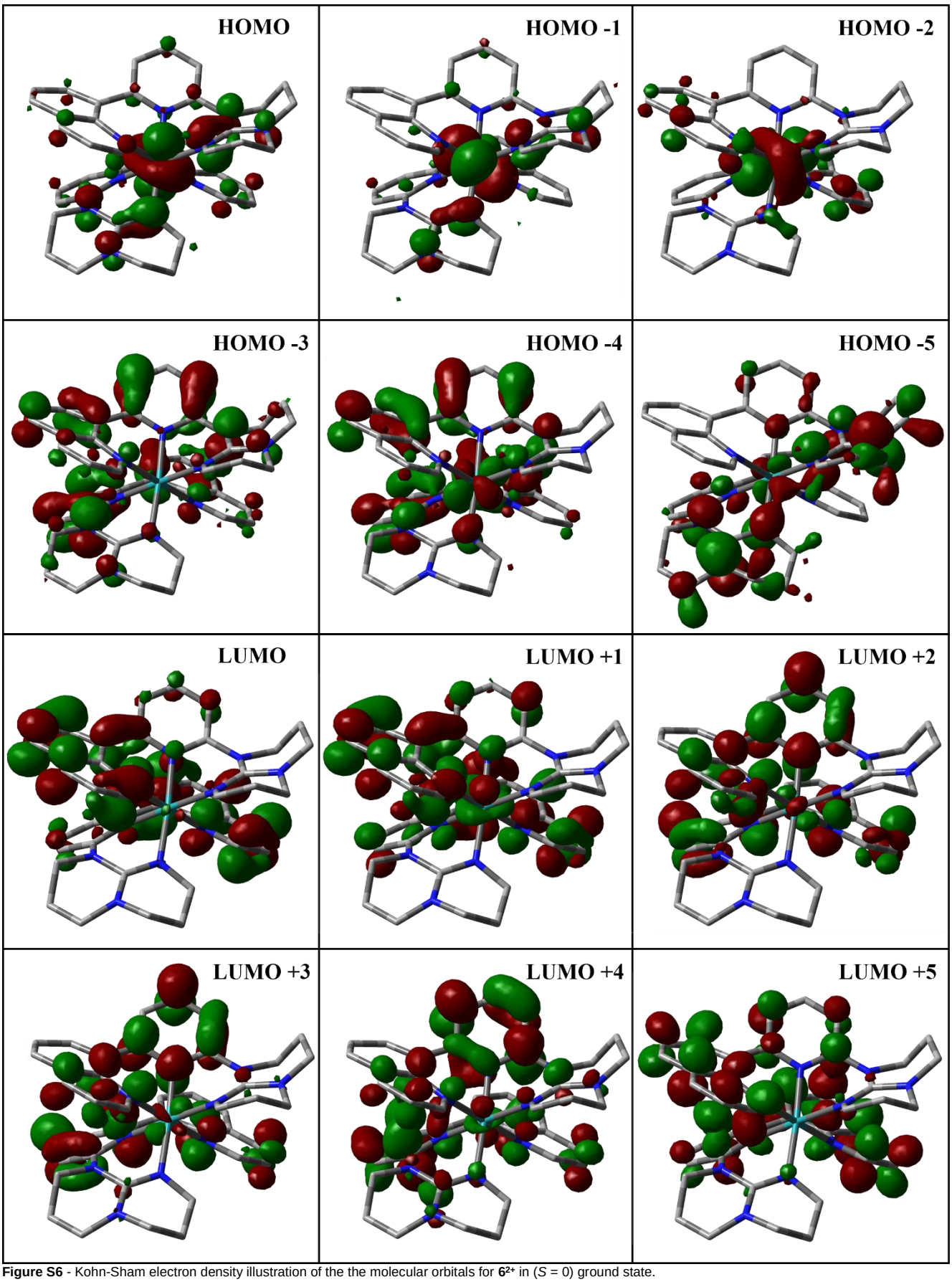

Figure S6 - Kohn-Sham electron density illustration of the the molecular orbitals for $\mathbf{6}^{2+}$ in (S = 0) ground state.

Table S17. MO composition of **6** in (*S=0*) ground state.

MO	Energy (eV)	Composition			
		Ruthenium	QpyG		
			Quinolyl	pyridyl	hpp
LUMO+5	-1.146	0	32	60	7
LUMO+4	-1.241	3	45	46	6
LUMO+3	-1.432	3	15	75	7
LUMO+2	-1.437	2	28	66	4
LUMO+1	-2.450	4	76	20	1
LUMO	**-2.559**	**1**	**80**	**18**	**1**
HOMO	**-5.225**	**65**	**3**	**5**	**28**
HOMO-1	-5.634	72	4	3	21
HOMO-2	-5.872	84	12	2	3
HOMO-3	-6.762	19	6	6	70
HOMO-4	-6.782	1	35	26	38
HOMO-5	-6.791	15	21	9	55

Table S18 - Selected transitions from TD-DFT calculations of **6^{2+}** in the singlet ground state (PBE0), CPCM (CH_3CN).

Energy (eV)	**λ (nm)**	**f**	**Transition**	**Character**
1.77	699	0.0697	HOMO→LUMO (98%)	Ru to quino; hpp to quino
2.50	496	0.1017	H-2→LUMO (87%)	Ru to quino; Ru to py
2.58	480	0.0758	HOMO→L+2 (87%)	hpp to py and/or quino; Ru to py and/or quino
3.64	341	0.3708	H-4→LUMO (35%) H-3→L+1 (40%) H-1→L+4 (15%)	Ru to quino; hpp to quino
4.26	291	0.1118	H-3→L+3 (78%)	hpp to py
4.39	282	0.0679	H-8→LUMO (29%) HOMO→L+8 (33%)	hpp to py and/or quino; Ru to py and/or quino
4.81	258	0.0898	HOMO→L+11 (44%) HOMO→L+15 (23%)	Ru to py; Ru to hpp; Ru to quino
5.10	243	0.1071	H-11→LUMO (44%) H-5→L+4 (12%) H-3→L+7 (16%)	hpp to quino
5.23	237	0.1199	H-11→LUMO (11%) H-6→L+5 (31%) H-4→L+6 (15%) H-3→L+7 (11%)	Ru to quino; hpp to quino
5.25	236	0.1895	H-6→L+5 (44%)	hpp to py; hpp to quino
5.33	232	0.1281	H-8→L+3 (13%) H-7→L+2 (36%) H-1→L+11 (22%)	Ru to py; hpp to py
5.35	232	0.1111	H-7→L+3 (11%) H-1→L+9 (11%) H-1→L+10 (29%) H-1→L+14 (26%)	Ru to py; Ru to quino
5.47	227	0.1088	H-10→L+2 (44%) H-9→L+3 (28%)	quino to py
5.48	226	0.0656	H-9→L+2 (10%) H-5→L+7 (57%)	hpp to py; hpp to quino
5.71	217	0.0687	H-8→L+4 (79%)	hpp to py and/or quino ; Ru to py and/or quino
5.86	212	0.1836	H-16→L+1 (10%) H-7→L+5 (52%)	hpp to py; hpp to quino
5.99	207	0.0650	H-12→L+3 (32%) H-8→L+6 (35%)	hpp to py; hpp to quino
6.01	206	0.1207	H-16→L+1 (14%) H-12→L+3 (35%) H-8→L+6 (28%)	hpp to quino
6.14	202	0.4772	H-10→L+5 (29%) H-7→L+7 (25%)	hpp to py

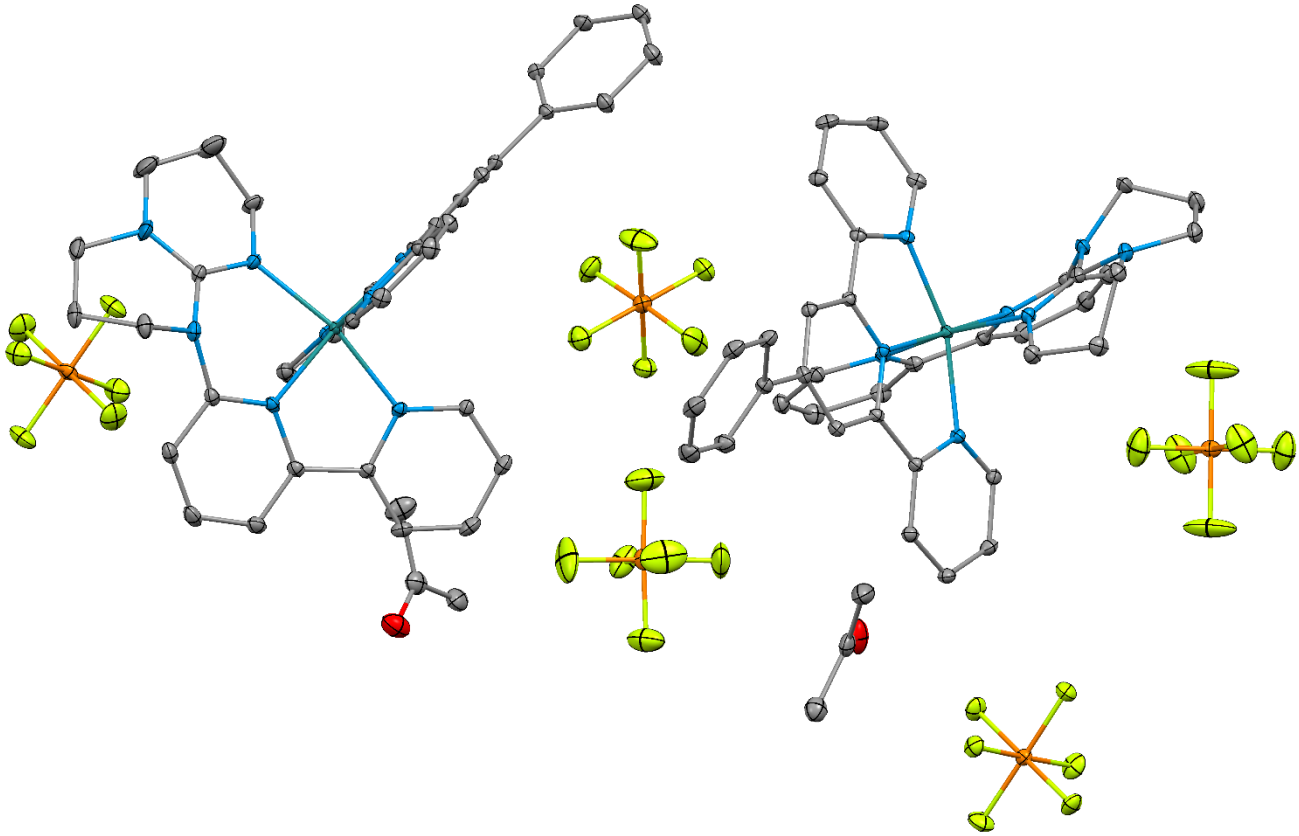

Figure S7 – Thermal ellipsoid diagram (30% probability) of the single crystal of **7** with the counter-anions (PF_6) and co-crystallized acetone solvent molecules. The hydrogens atoms are omitted for clarity.

Table S19 – Atomic coordinates for DFT optimization of $\mathbf{7}^{2+}$ in (*S* = 0) PBE0/LANL2DZ, CPCM(CH_3CN).

Standard orientation					
Center Number	Atomic Number	Atomic Type	Coordinates (Angstroms)		
			X	Y	Z
1	44	0	-0.654055	0.368963	0.124550
2	7	0	-2.633813	0.863454	0.239355
3	7	0	-0.375048	-0.609646	1.922699
4	7	0	1.291900	0.057585	0.058551
5	7	0	-0.528905	2.273126	0.915780
6	7	0	-0.189507	1.220156	-1.724807
7	7	0	-1.152294	-1.427787	-0.820646
8	7	0	-3.398286	-1.383749	-0.021375
9	6	0	1.887209	-0.594997	1.095246
10	6	0	1.161977	1.205931	-2.005646
11	6	0	2.005797	0.539397	-0.996201
12	6	0	-3.655385	-0.001670	0.022735
13	6	0	0.934355	-0.987725	2.147107
14	7	0	-2.580005	-3.300934	-1.081470
15	6	0	-1.315417	-0.913535	2.847914
16	1	0	-2.325256	-0.590261	2.630817

17	6	0	-2.891712	2.188589	0.496701
18	6	0	-1.710734	2.970264	0.890040
19	6	0	3.388568	0.357189	-1.042263
20	1	0	3.956128	0.712250	-1.893614
21	6	0	0.599067	2.895723	1.337308
22	1	0	1.505715	2.305425	1.351199
23	6	0	-2.327531	-2.017185	-0.675497
24	6	0	1.293504	-1.682705	3.307442
25	1	0	2.323205	-1.977148	3.470940
26	6	0	0.767835	2.365076	-4.091755
27	1	0	1.140144	2.811446	-5.006942
28	6	0	-1.010453	-1.603675	4.023285
29	1	0	-1.798375	-1.824940	4.733402
30	6	0	-1.759970	4.318060	1.271393
31	1	0	-2.695421	4.862619	1.244320
32	6	0	-4.442908	-2.298440	0.500426
33	1	0	-5.184583	-1.718746	1.048124
34	1	0	-3.970885	-2.982041	1.216513
35	6	0	1.656301	1.778382	-3.181990
36	1	0	2.719065	1.766060	-3.391466
37	6	0	-3.912797	-3.917926	-1.264522
38	1	0	-3.876706	-4.895787	-0.769771
39	1	0	-4.078215	-4.094472	-2.334999
40	6	0	0.314809	-1.997101	4.256929
41	1	0	0.581580	-2.536355	5.158821
42	6	0	-1.042706	1.780956	-2.610518
43	1	0	-2.093932	1.756881	-2.351417
44	6	0	-4.190120	2.698238	0.453616
45	1	0	-4.387120	3.742220	0.658421
46	6	0	-4.978167	0.475774	-0.075956
47	1	0	-5.785737	-0.198162	-0.329822
48	6	0	-0.603314	2.362573	-3.803714
49	1	0	-1.324083	2.800870	-4.483560
50	6	0	-0.592812	4.959299	1.696453
51	1	0	-0.619162	6.001552	1.993624
52	6	0	4.044902	-0.321642	0.008094
53	6	0	3.269391	-0.796420	1.088132
54	1	0	3.750811	-1.291705	1.922587
55	6	0	7.478854	-1.863964	0.534329
56	1	0	7.906397	-2.757801	0.978258
57	6	0	-0.587117	-3.244208	-2.477318
58	1	0	0.275145	-3.805430	-2.850506
59	1	0	-1.181386	-2.923348	-3.340916
60	6	0	0.605888	4.232126	1.737365
61	1	0	1.531861	4.686846	2.068510

62	6	0	5.512071	-0.524029	-0.020070
63	6	0	-1.448926	-4.109396	-1.566071
64	1	0	-1.854356	-4.972241	-2.098474
65	1	0	-0.862247	-4.481427	-0.715720
66	6	0	-0.105159	-2.046077	-1.665976
67	1	0	0.716548	-2.356612	-1.009094
68	1	0	0.288931	-1.276745	-2.336131
69	6	0	-5.039054	-3.076980	-0.664319
70	1	0	-5.452185	-2.380843	-1.402123
71	1	0	-5.850431	-3.730184	-0.330590
72	6	0	6.091724	-1.671923	0.560752
73	1	0	5.460756	-2.433453	1.009969
74	6	0	-5.240187	1.829728	0.130942
75	1	0	-6.254298	2.203558	0.047765
76	6	0	7.746809	0.235950	-0.651980
77	1	0	8.384116	0.982961	-1.115250
78	6	0	6.359458	0.426999	-0.627546
79	1	0	5.943488	1.333526	-1.058052
80	6	0	8.312988	-0.910564	-0.071615
81	1	0	9.388380	-1.058868	-0.091165

Table S20 - Selected bond distances and angles of **7**

Bond Length			**Angle**		
	Obs. (X-ray)	**Calc. (DFT)**		**Obs. (X-ray)**	**Calcl. (DFT)**
N1-Ru1	**2.072 (2)**	**2.06612**	**N1-Ru1-N2**	**79.55 (8)**	**79.692**
			N1-Ru1-N3	**159.00 (8)**	**159.035**
N2-Ru1	**1.957 (2)**	**1.97181**	**N1-Ru1-N4**	**83.87 (8)**	**87.134**
			N1-Ru1-N5	**100.39 (8)**	**101.333**
N3-Ru1	**2.059 (2)**	**2.08817**	**N1-Ru1-N7**	**91.61 (8)**	**91.065**
			N2-Ru1-N3	**79.87 (8)**	**79.349**
N4-Ru1	**2.048 (2)**	**2.06580**	**N2-Ru1-N4**	**97.31 (8)**	**95.658**
			N2-Ru1-N5	**176.59 (8)**	**174.903**
N5-Ru1	**2.026 (2)**	**2.04381**	**N2-Ru1-N7**	**93.95 (8)**	**94.839**
			N3-Ru1-N4	**94.63 (8)**	**95.455**
N7-Ru1	**2.076 (2)**	**2.09044**	**N3-Ru1-N5**	**99.91 (8)**	**99.591**
			N3-Ru1-N7	**93.95 (8)**	**90.168**
N9-Ru2	**2.071 (2)**	**2.06612**	**N4-Ru1-N5**	**79.31 (9)**	**79.920**
			N4-Ru1-N7	**166.89 (8)**	**168.485**
N10-Ru2	**1.960 (2)**	**1.97181**	**N5-Ru1-N7**	**89.46 (9)**	**90.142**
			N9-Ru2-N10	**79.73 (8)**	**79.692**
N11-Ru2	**2.066 (2)**	**2.08817**	**N9-Ru2-N11**	**159.38 (8)**	**159.035**
			N9-Ru2-N12	**86.30 (8)**	**87.134**
N12-Ru2	**2.056 (2)**	**2.06580**	**N9-Ru2-N13**	**100.02 (8)**	**101.333**
			N9-Ru2-N15	**88.65 (8)**	**91.065**
N13-Ru2	**2.032 (2)**	**2.04381**	**N10-Ru2-N11**	**79.65 (9)**	**79.349**
			N10-Ru2-N12	**96.19 (8)**	**95.658**
N15-Ru2	**2.084 (2)**	**2.09044**	**N10-Ru2-N13**	**175.40 (8)**	**174.903**
			N10-Ru2-N15	**95.10 (8)**	**94.839**
			N11-Ru2-N12	**95.57 (8)**	**95.455**
			N11-Ru2-N13	**100.50 (8)**	**99.591**
			N11-Ru2-N15	**93.53 (8)**	**90.168**
			N12-Ru2-N13	**79.22 (9)**	**79.920**
			N12-Ru2-N15	**166.61 (8)**	**168.485**
			N13-Ru2-N15	**89.48 (9)**	**90.142**

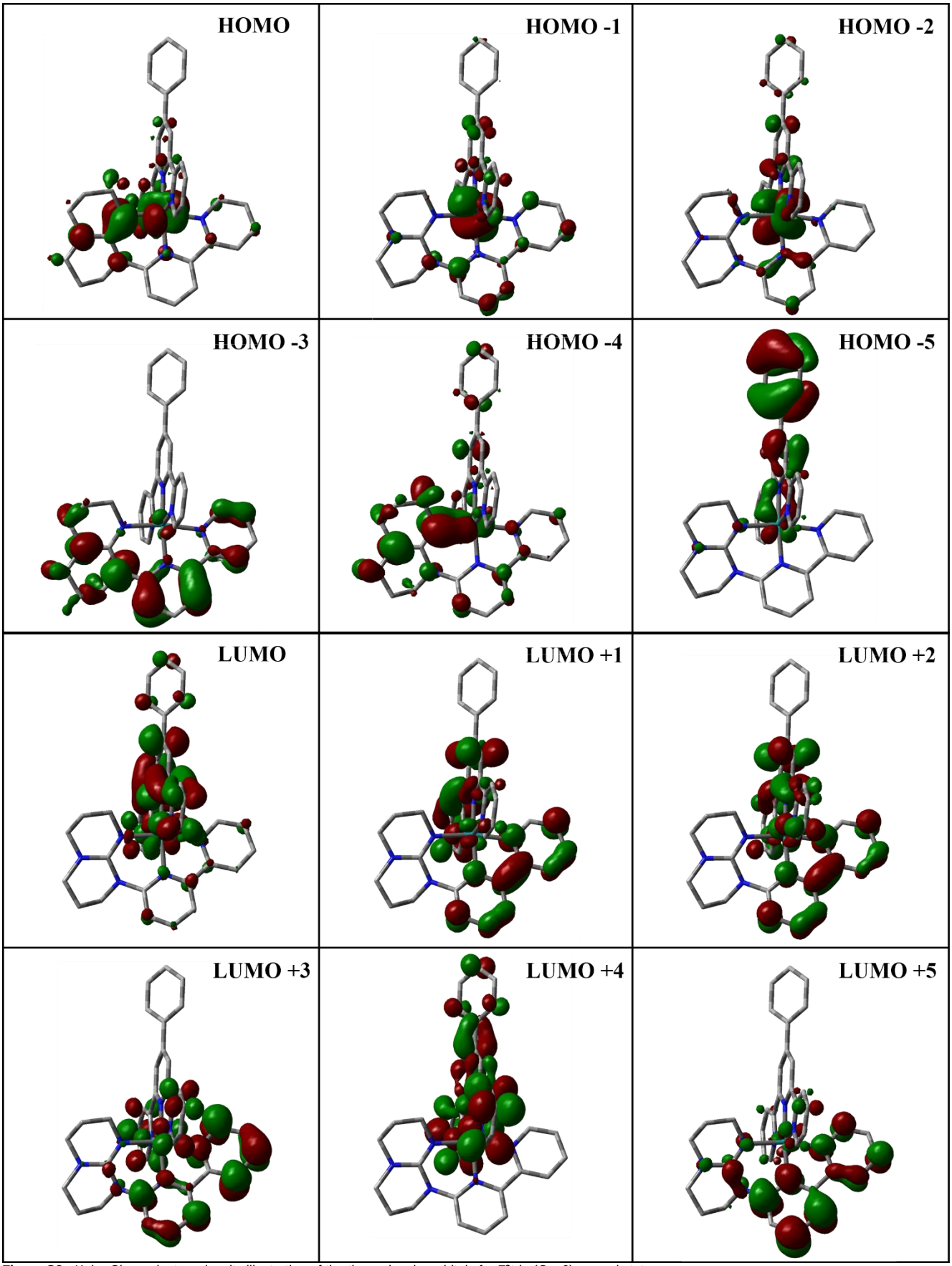

Figure S8 - Kohn-Sham electron density illustration of the the molecular orbitals for **7**$^{2+}$ in (*S* = 0) ground state.

Table S21. MO composition of **7** in (*S=0*) ground state.

MO	Energy (eV)	Composition			
		Ruthenium	Phtpy	bpyhpp	
				2,2'-bipyridyl	hpp
LUMO+5	-1.442	2	10	82	6
LUMO+4	-1.592	0	97	2	0
LUMO+3	-1.613	1	31	65	2
LUMO+2	-2.444	6	53	41	0
LUMO+1	-2.554	3	53	44	0
LUMO	**-2.731**	**7**	**83**	**9**	**1**
HOMO	**-5.822**	**54**	**13**	**5**	**26**
HOMO-1	-6.302	67	17	13	4
HOMO-2	-6.425	74	17	6	3
HOMO-3	-7.203	3	1	45	46
HOMO-4	-7.247	13	16	10	52
HOMO-5	-7.620	8	87	2	3

Table S22 - Selected transitions from TD-DFT calculations of **7^{2+}** in the singlet ground state (PBE0), CPCM (CH_3CN).

Energy (eV)	**λ (nm)**	**f**	**Transition**	**Character**
2.03	609	0.0232	H→L (89%)	hpp to tpy ; Ru to tpy
2.42	512	0.0201	H→L+1 (30%) H→L+2 (58%)	hpp to bpy &/or hpp to tpy ; Ru to bpy &/or Ru to tpy
2.69	461	0.1855	H-2→L (45%) H-1→L (22%) H-1→L+2 (20%)	Ru to bpy ; Ru to tpy
2.83	439	0.0901	H-2→L+1 (18%) H-1→L+1 (63%)	Ru to bpy ; Ru to tpy
3.05	407	0.0232	H-2→L (10%) H-1→L+2 (62%)	Ru to bpy ; Ru to tpy
3.39	366	0.0782	H→L+4 (80%)	hpp to bpy &/or hpp to tpy ; Ru to bpy &/or Ru to tpy
4.13	300	0.1472	H-6→L (19%) H-3→L+2 (35%)	hpp to bpy &/or hpp to tpy ; Ru to bpy &/or Ru to tpy
4.18	296	0.2858	H-6→L (15%) H-5→L (39%)	hpp to bpy &/or hpp to tpy ; Ru to bpy &/or Ru to tpy
4.26	291	0.2005	H-6→L (18%) H-5→L (48%)	Ru to bpy ; Ru to tpy
4.64	267	0.1589	H-6→L+2 (22%) H-5→L+1 (10%) H-5→L+2 (33%)	tpy to bpy
4.65	267	0.1825	H-6→L+2 (37%) H-5→L+1 (18%) H-5→L+2 (20%)	tpy to bpy
4.99	249	0.1126	H-8→L+1 (34%) H-3→L+4 (41%)	hpp to tpy ; bpy to tpy
4.99	248	0.1285	H-8→L+1 (11%) H-4→L+5 (29%) H-3→L+4 (27%) H-3→L+5 (11%)	hpp to tpy ; hpp to bpy
5.21	238	0.1311	H-9→L+1 (47%)	hpp to bpy ; tpy to bpy

Table S23 – Atomic coordinates for DFT optimization of $\mathbf{8}^{2+}$ in (S = 0) PBE0/LANL2DZ, CPCM(CH_3CN).

Standard orientation					
Center Number	Atomic Number	Atomic Type	Coordinates (Angstroms)		
			X	Y	Z
1	44	0	-0.556957	-0.178514	0.005764
2	6	0	-4.908829	-0.001579	0.266023
3	6	0	-5.249301	-1.316149	0.011031
4	7	0	-2.580600	-0.470827	-0.047601
5	6	0	-4.245547	-2.248727	-0.350821
6	6	0	-3.549328	0.432086	0.201168
7	6	0	-2.919753	-1.772429	-0.354237
8	6	0	-4.502477	-3.614354	-0.713516
9	6	0	-3.478637	-4.446249	-1.094029
10	6	0	-2.122171	-3.970853	-1.137518
11	6	0	-1.026395	-4.766692	-1.557393
12	6	0	-1.853483	-2.635031	-0.751971
13	6	0	0.246583	-4.210110	-1.581209
14	6	0	0.434773	-2.871233	-1.180983
15	7	0	-0.585143	-2.097297	-0.771964
16	7	0	-3.255893	1.807769	0.317106
17	6	0	-4.045833	4.162413	-0.092440
18	7	0	-2.084967	3.663978	1.218529
19	6	0	-3.331050	4.444760	1.218359
20	6	0	-2.051806	2.353527	0.816320
21	6	0	-4.405826	2.689112	-0.072842
22	7	0	-0.943331	1.633865	0.940331
23	6	0	0.410060	3.661483	1.221395
24	6	0	-0.859916	4.483630	1.392320
25	6	0	0.115288	2.263043	1.755951
26	1	0	-3.395675	4.418399	-0.935866
27	1	0	-4.968882	4.742306	-0.182972
28	1	0	-5.690678	0.692884	0.533096
29	1	0	-4.769177	2.351632	-1.047901
30	1	0	-6.286117	-1.629138	0.077514
31	1	0	-5.526728	-3.973570	-0.691338
32	1	0	-3.678429	-5.475210	-1.376534
33	1	0	-1.189637	-5.796288	-1.859005
34	1	0	1.105808	-4.787097	-1.901599
35	1	0	1.420898	-2.425086	-1.193056
36	1	0	-5.209855	2.565927	0.659697
37	1	0	-3.961237	4.174812	2.075276
38	1	0	-3.065085	5.498236	1.319994
39	1	0	-0.894876	5.308526	0.669332
40	1	0	-0.899885	4.919819	2.397309
41	1	0	1.232624	4.133538	1.767195

42	1	0	0.700165	3.591799	0.167425
43	1	0	-0.214773	2.328866	2.803520
44	1	0	1.002786	1.636185	1.729465
45	7	0	-0.254170	0.747060	-1.817727
46	6	0	0.478384	2.015954	-4.206064
47	6	0	1.077153	0.979791	-2.102876
48	6	0	-1.195819	1.137919	-2.708518
49	6	0	-0.870124	1.773304	-3.909032
50	6	0	1.457897	1.612432	-3.291613
51	7	0	1.409990	-0.053251	-0.004063
52	6	0	4.187434	0.041451	-0.067968
53	6	0	2.026750	0.511247	-1.079441
54	6	0	2.113867	-0.579073	1.038053
55	6	0	3.509212	-0.541879	1.024913
56	6	0	3.421398	0.569304	-1.129834
57	7	0	-0.108989	-1.015436	1.863224
58	6	0	0.815162	-2.138095	4.252852
59	6	0	-0.981314	-1.453085	2.798346
60	6	0	1.245865	-1.117621	2.102450
61	6	0	1.723488	-1.679600	3.291069
62	6	0	-0.558981	-2.019707	4.004429
63	6	0	5.667371	0.095982	-0.099561
64	6	0	8.492061	0.203663	-0.159721
65	6	0	6.439455	-0.924906	0.494432
66	6	0	6.333914	1.171691	-0.723563
67	6	0	7.733173	1.225780	-0.752352
68	6	0	7.838815	-0.872097	0.463267
69	1	0	8.417204	-1.671134	0.916942
70	1	0	9.576795	0.244949	-0.182677
71	1	0	8.229083	2.066123	-1.228498
72	1	0	5.763505	1.984734	-1.163315
73	1	0	5.952186	-1.778121	0.957778
74	1	0	4.072754	-0.934795	1.862430
75	1	0	3.917119	0.995178	-1.993717
76	1	0	2.789040	-1.756904	3.469751
77	1	0	1.174531	-2.575450	5.177540
78	1	0	-2.033275	-1.341339	2.566931
79	1	0	-1.294237	-2.358010	4.724702
80	1	0	2.505195	1.790389	-3.504271
81	1	0	0.762368	2.508253	-5.129289
82	1	0	-1.659992	2.068776	-4.589369
83	1	0	-2.224762	0.929796	-2.444207

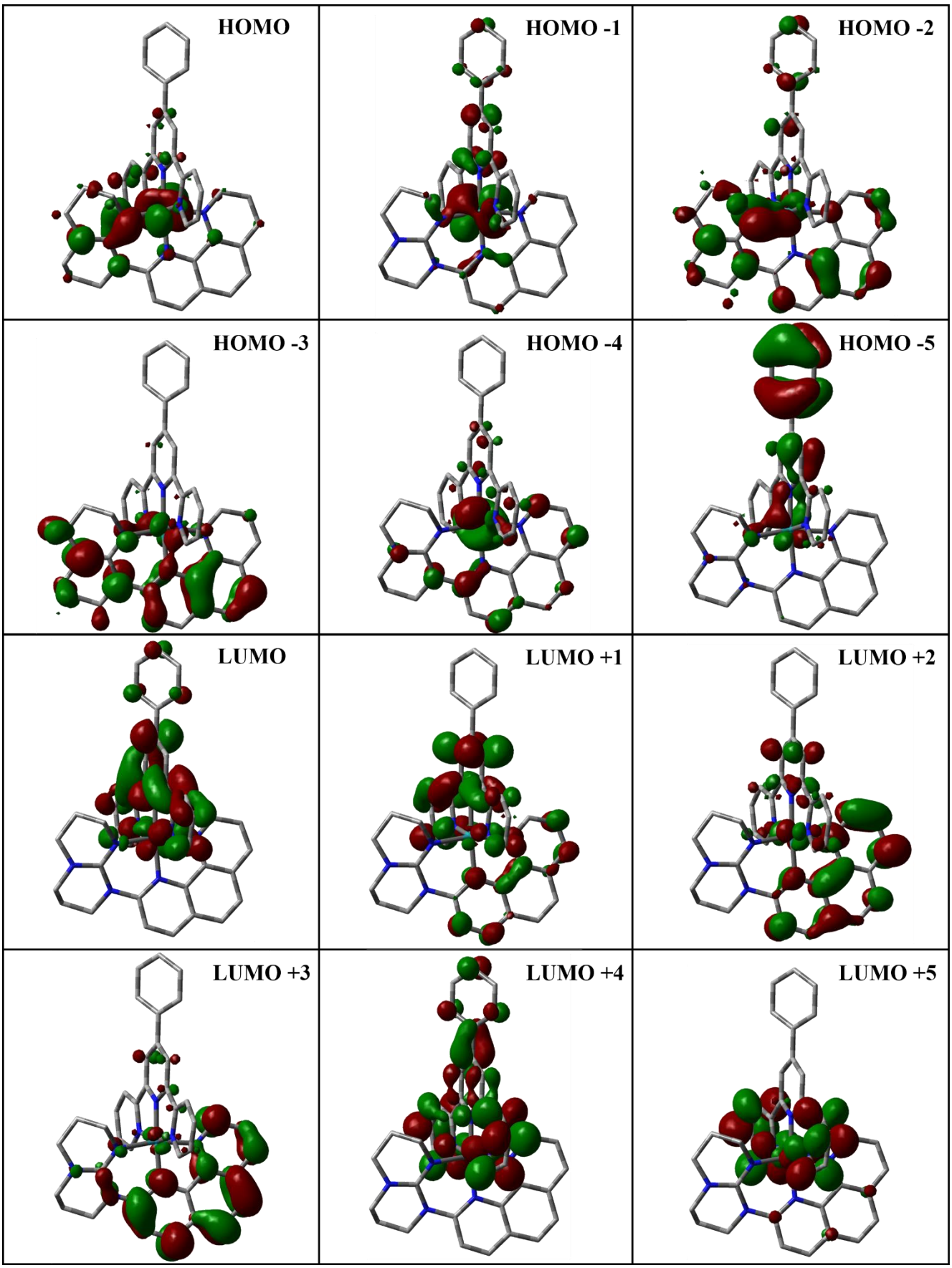

Figure S9 - Kohn-Sham electron density illustration of the the molecular orbitals for $\mathbf{8}^{2+}$ in (S = 0) ground state.

Table S24. MO composition of **8** in (*S=0*) ground state.

MO	Energy (eV)	Composition			
		Ruthenium	Phtpy	phenG	
				1,10-phenanthroline	hpp
LUMO+5	-1.205	2	90	7	1
LUMO+4	-1.238	1	98	1	0
LUMO+3	-2.261	3	14	82	0
LUMO+2	-2.308	2	59	37	3
LUMO+1	-2.325	3	64	32	1
LUMO	**-2.421**	**1**	**58**	**38**	**2**
HOMO	**-5.599**	**61**	**8**	**3**	**28**
HOMO-1	-6.080	71	8	14	7
HOMO-2	-6.284	83	10	4	3
HOMO-3	-7.129	9	2	39	49
HOMO-4	-7.193	19	5	22	54
HOMO-5	-7.621	0	92	5	2

Table S25- Selected transitions from TD-DFT calculations of $\mathbf{8^{2+}}$ in the singlet ground state (PBE0), CPCM (CH_3CN).

Energy (eV)	**λ (nm)**	**f**	**Transition**	**Character**
2,00	620	0,0222	HOMO→LUMO (92%)	hpp to tpy ; Ru to tpy
2,31	536	0,0106	HOMO→L+1 (47%) HOMO→L+2 (38%)	hpp to tpy and/or phen ; Ru to tpy and/or phen
2,38	520	0,0174	H-1→LUMO (34%) HOMO→L+1 (19%) HOMO→L+2 (41%)	hpp to tpy and/or phen ; Ru to tpy and/or phen
2,62	474	0,0023	HOMO→L+3 (88%)	hpp to phen ; Ru to phen
2,68	463	0,1446	H-2→LUMO (53%) H-1→L+2 (19%)	Ru to tpy; Ru to phen
2,80	443	0,1314	H-1→L+1 (86%)	Ru to tpy
2,85	435	0,0165	H-2→L+1 (37%) H-2→L+2 (52%)	Ru to tpy; Ru to phen
2,89	428	0,0244	H-2→L+1 (56%) H-2→L+2 (36%)	Ru to tpy; Ru to phen
3,03	409	0,0762	H-2→LUMO (10%) H-1→L+2 (62%)	Ru to tpy; Ru to phen
3,13	396	0,0351	H-2→L+3 (10%) H-1→L+3 (81%)	Ru to phen
3,22	386	0,0291	H-2→L+3 (74%)	Ru to phen
3,35	370	0,081	HOMO→L+4 (91%)	Ru to tpy; hpp to tpy
4,63	268	0,1625	H-6→L+1 (15%) H-6→L+2 (52%)	tpy to phen
4,67	265	0,1307	HOMO→L+9 (60%)	Ru to phen; hpp to phen
5,43	228	0,2827	H-11→LUMO (15%) H-9→L+3 (52%)	hpp to phen; hpp to tpy
5,56	223	0,2513	H-4→L+7 (10%) H-3→L+7 (38%)	hpp to phen

Table S26 – Atomic coordinates for DFT optimization of $\mathbf{9^{3+}}$ in (*S* = 1) PBE0/LANL2DZ, CPCM(CH_3CN).

Standard orientation					
Center Number	Atomic Number	Atomic Type	Coordinates (Angstroms)		
			X	Y	Z
1	44	0	0.658189	0.062898	-0.036072
2	7	0	2.735650	0.051053	-0.076768
3	7	0	0.297281	-1.107042	-1.744856

4	7	0	-1.330971	0.034689	-0.052956
5	7	0	0.230981	1.339338	1.561271
6	7	0	0.739799	-1.508696	1.202729
7	7	0	2.622982	-2.343027	0.038204
8	6	0	-1.958201	-0.775320	-0.944918
9	6	0	-1.119328	1.573103	1.727383
10	6	0	-2.005560	0.810749	0.831877
11	6	0	3.378470	-1.148977	-0.020384
12	6	0	-1.034055	-1.435070	-1.892343
13	7	0	1.368654	-3.782316	1.393727
14	6	0	1.197911	-1.547027	-2.648547
15	6	0	3.463765	1.209734	-0.188394
16	6	0	-3.401166	0.778763	0.855057
17	6	0	1.564971	-2.541556	0.913169
18	6	0	-1.450624	-2.276652	-2.924000
19	6	0	-0.656370	3.076160	3.561798
20	6	0	0.833215	-2.379391	-3.711511
21	6	0	3.164418	-3.569485	-0.602666
22	6	0	-1.577878	2.448240	2.714402
23	6	0	2.307632	-4.923647	1.263255
24	6	0	-0.506106	-2.764314	-3.838826
25	6	0	1.114181	1.928318	2.397240
26	6	0	4.861444	1.151241	-0.301601
27	6	0	4.777226	-1.238380	-0.057044
28	6	0	0.707688	2.801385	3.410074
29	6	0	-4.096972	-0.064568	-0.038153
30	6	0	-3.348369	-0.846627	-0.950559
31	6	0	-7.639705	-1.381909	-0.373294
32	6	0	-0.025880	-2.889694	3.168024
33	6	0	-5.573104	-0.128459	-0.028720
34	6	0	0.157458	-4.048770	2.198554
35	6	0	-0.187110	-1.607186	2.358389
36	6	0	3.565201	-4.562850	0.480640
37	6	0	-6.241534	-1.319443	-0.385792
38	6	0	5.522771	-0.074793	-0.214727
39	6	0	-7.737896	0.937120	0.342106
40	6	0	-6.339645	0.998790	0.337156
41	6	0	-8.393446	-0.253618	-0.011275
42	6	0	-0.613157	3.362784	-2.571450
43	6	0	0.155462	4.421510	-2.129625
44	7	0	0.693927	1.814184	-1.247978
45	6	0	1.273098	4.174998	-1.286938
46	6	0	-0.332826	2.076355	-2.070563
47	6	0	1.586280	2.823128	-0.927287
48	6	0	2.079149	5.244392	-0.811984

49	6	0	3.180304	4.977589	-0.021863
50	6	0	3.559806	3.637788	0.218091
51	6	0	2.821989	2.548554	-0.255777
52	1	0	-0.986797	1.255471	-2.329871
53	1	0	-1.453554	3.500019	-3.239733
54	1	0	-0.075122	5.441290	-2.421053
55	1	0	1.811492	6.262796	-1.075853
56	1	0	3.784099	5.782870	0.380605
57	1	0	4.465620	3.458953	0.787189
58	1	0	5.427274	2.055471	-0.477155
59	1	0	6.604330	-0.120342	-0.267214
60	1	0	5.271527	-2.194282	0.048315
61	1	0	3.990730	-3.294463	-1.255724
62	1	0	3.989014	-5.467977	0.038112
63	1	0	4.324386	-4.123668	1.135812
64	1	0	2.375191	-3.991887	-1.235331
65	1	0	2.555662	-5.266099	2.273384
66	1	0	1.758871	-5.728437	0.761310
67	1	0	0.308807	-4.993470	2.722631
68	1	0	-0.709112	-4.159593	1.535721
69	1	0	-0.916157	-3.038509	3.785064
70	1	0	0.840827	-2.832640	3.835285
71	1	0	-1.210106	-1.550227	1.971511
72	1	0	-0.024323	-0.735680	2.997585
73	1	0	2.157753	1.682698	2.258408
74	1	0	1.450809	3.248686	4.058460
75	1	0	-1.001006	3.756523	4.331847
76	1	0	-2.637682	2.636505	2.830847
77	1	0	2.220132	-1.217276	-2.520827
78	1	0	1.587334	-2.710898	-4.414301
79	1	0	-0.818410	-3.418681	-4.644494
80	1	0	-2.494776	-2.543948	-3.027835
81	1	0	-3.859268	-1.468675	-1.674020
82	1	0	-8.139057	-2.308259	-0.638948
83	1	0	-5.676208	-2.210254	-0.643655
84	1	0	-3.948253	1.371059	1.577164
85	1	0	-5.851483	1.935945	0.587679
86	1	0	-8.314057	1.815914	0.613830
87	1	0	-9.477979	-0.301505	-0.004997

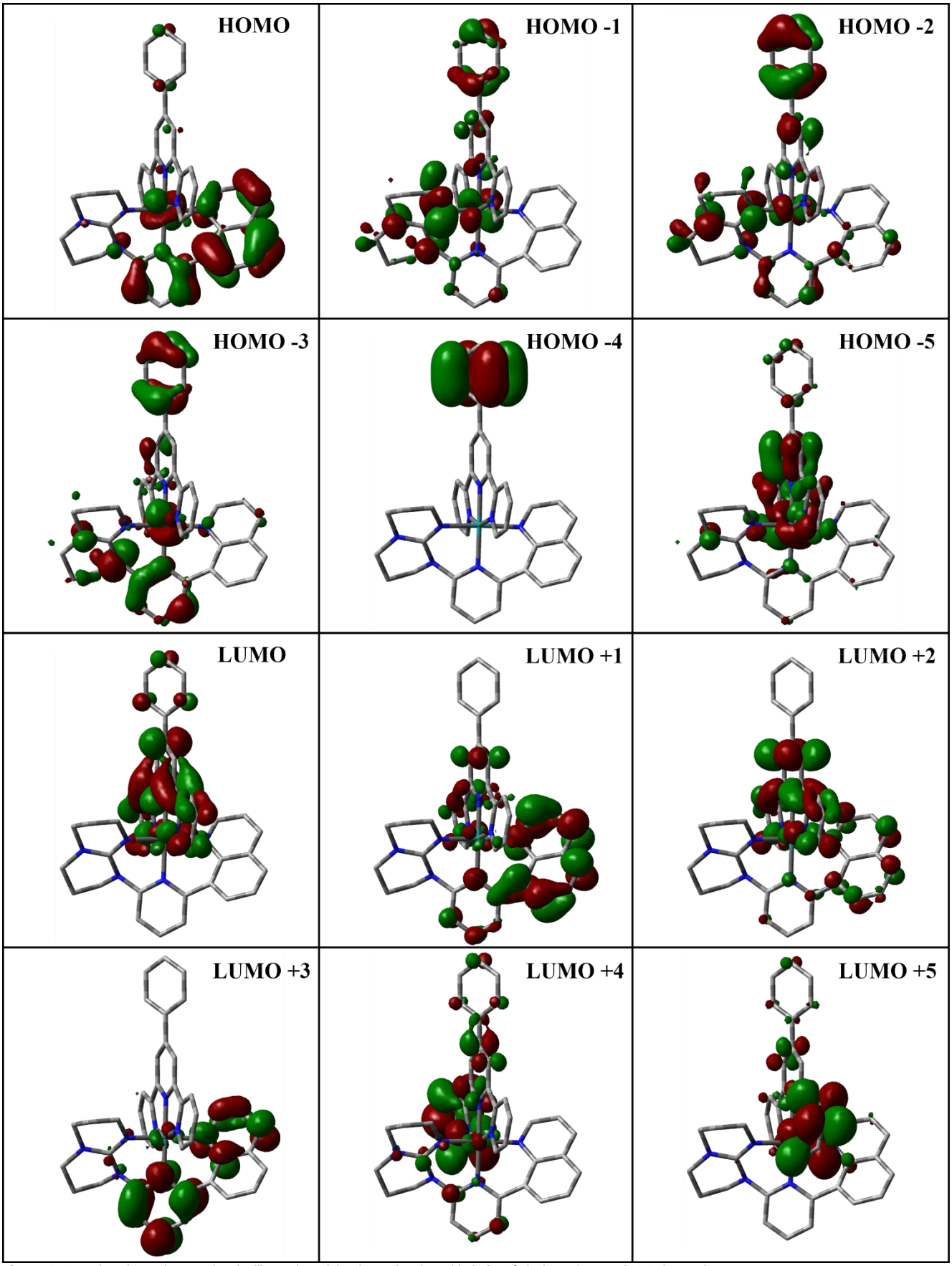

Figure S10 - Kohn-Sham electron density illustration of the the molecular orbitals for $\mathbf{9}^{3+}$ in (S = 1) ground state in α-spin

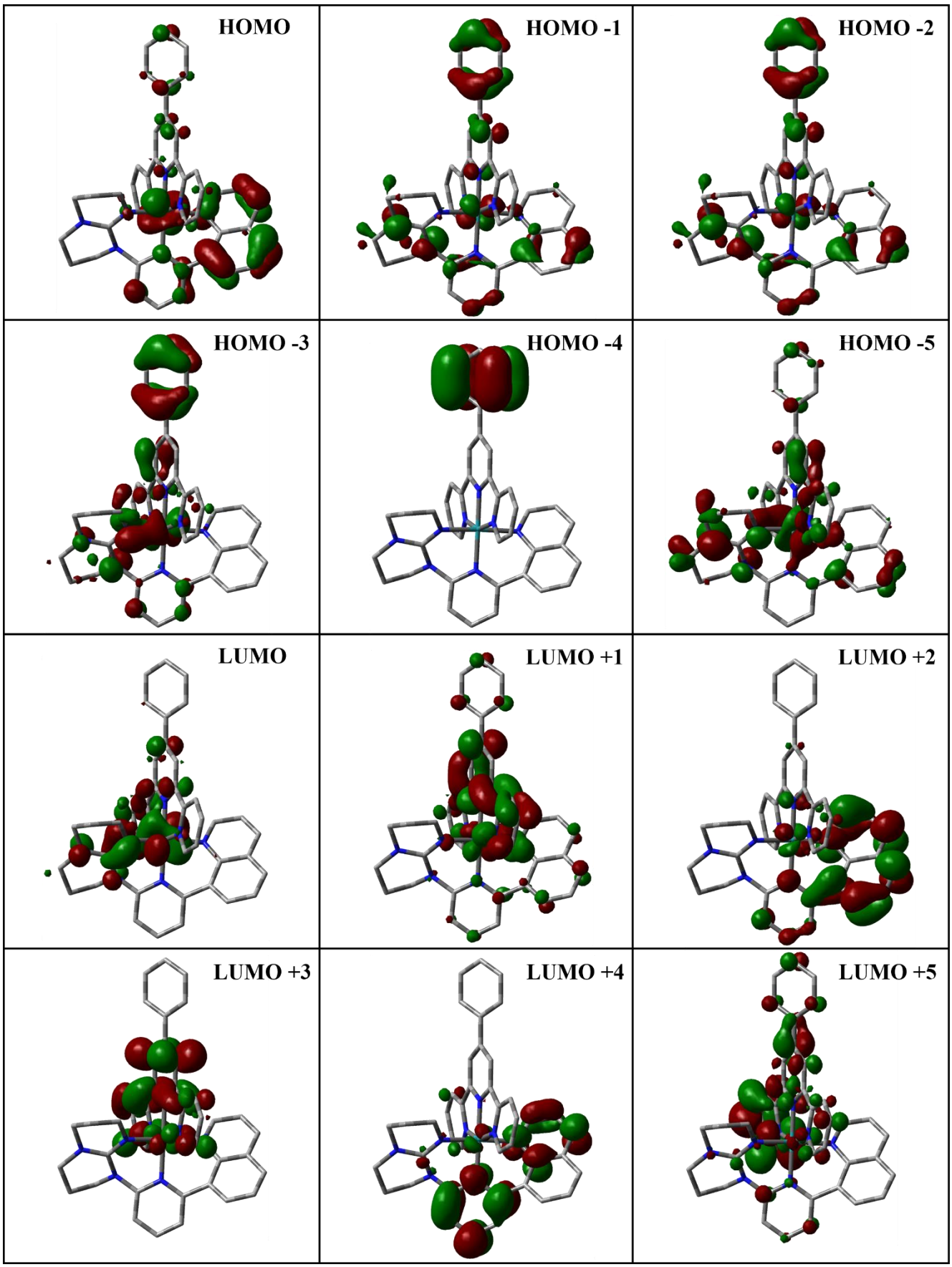

Figure S11 - Kohn-Sham electron density illustration of the the molecular orbitals for $\mathbf{9}^{3+}$ in (S = 1) ground state in β-spin

Table S27. MO composition of **9** in (*S=1*) ground state in α-spin.

MO	Energy (eV)	Composition				
		Ruthenium	Phtpy	QpyG		
				Quino	py	hpp
LUMO+5	-2.061	42	7	18	21	11
LUMO+4	-2.083	2	2	13	72	11
LUMO+3	-2.686	55	34	4	4	3
LUMO+2	-2.853	3	87	7	2	0
LUMO+1	-2.949	6	91	2	0	0
LUMO	**-3.089**	**3**	**13**	**65**	**19**	**1**
HOMO	**-7.398**	**4**	**1**	**58**	**26**	**10**
HOMO-1	-7.556	12	3	0	0	84
HOMO-2	-7.748	6	83	1	3	7
HOMO-3	-7.822	100	0	0	0	0
HOMO-4	-7.909	16	21	13	15	35
HOMO-5	-8.069	1	95	1	1	2

Table S28. MO composition of **9** in (*S=1*) ground state in β-spin.

MO	Energy (eV)	Composition				
		Ruthenium	Phtpy	QpyG		
				Quino	py	hpp
LUMO+5	-2.047	2	2	15	72	9
LUMO+4	-2.373	60	29	4	3	4
LUMO+3	-2.833	4	81	13	2	0
LUMO+2	-2.864	4	94	1	0	1
LUMO+1	-3.079	1	16	64	18	1
LUMO	**-4.758**	**67**	**10**	**1**	**3**	**19**
HOMO	**-7.321**	**17**	**3**	**45**	**17**	**17**
HOMO-1	-7.447	14	3	9	15	60
HOMO-2	-7.746	15	81	0	1	2
HOMO-3	-7.820	0	100	0	0	0
HOMO-4	-7.898	29	26	9	9	25
HOMO-5	-8.013	29	51	5	2	13

Table S29- Selected transitions from TD-DFT calculations of $\mathbf{9^{3+}}$ in (*S=1*) ground state (PBE0), CPCM (CH_3CN).

Energy (eV)	λ (nm)	f	Transition	Character
2.02	614	0.0079	H-3(β)→LUMO(β) (12%) H-1(β)→LUMO(β) (59%) HOMO(β)→LUMO(β) (22%)	tpy to Ru; py to Ru; Q to Ru
2.13	581	0.1432	H-5(β)→LUMO(β) (30%) H-3(β)→LUMO(β) (32%) H-1(β)→LUMO(β) (13%)	tpy to Ru; py to Ru; Q to Ru; hpp to Ru
2.44	508	0.0224	H-5(β)→LUMO(β) (30%) H-3(β)→LUMO(β) (12%) H-2(β)→LUMO(β) (13%)	py to Ru; Q to Ru; hpp to Ru
2.54	488	0.0325	H-6(β)→LUMO(β) (56%) H-3(β)→LUMO(β) (18%)	tpy to Ru
3.14	394	0.0675	HOMO(α)→LUMO(α) (24%) HOMO(β)→L+1(β) (19%)	Ru to tpy; py to tpy; Q to tpy; hpp to tpy
3.75	331	0.1043	H-3(β)→L+1(β) (22%)	Ru to tpy; hpp to tpy
4.01	309	0.0305	H-5(β)→L+1(β) (20%) H-1(β)→L+3(β) (17%)	Ru to tpy; hpp to tpy
4.02	309	0.0499	H-6(β)→L+1(β) (12%)	Ru to tpy and/or Ru to Q; hpp to tpy and/or hpp to Q
4.08	304	0.0444	H-12(β)→LUMO(β) (14%) H-6(β)→L+1(β) (16%) H-3(β)→L+3(β) (16%)	hpp to tpy
4.16	298	0.0602	H-12(β)→LUMO(β) (31%) H-3(β)→L+2(β) (12%)	tpy to Ru and/or tpy to Q; hpp to Ru and/or hpp to Q
4.32	287	0.0368	H-8(α)→LUMO(α) (30%)	Ru to tpy; hpp to tpy; Q to tpy
4.55	272	0.0434	H-1(α)→L+4(α) (12%)	Ru to tpy and/or Ru to Q and/or Ru to py; hpp to tpy and/or hpp to Q and/or hpp to py
4.59	270	0.0737	H-1(α)→L+5(α) (13%) HOMO(α)→L+4(α) (11%)	Ru to tpy; hpp to tpy; Q to tpy
4.64	267	0.0324	H-8(α)→L+1(α) (21%) H-8(β)→L+2(β) (30%)	Ru to py and/or hpp to py; Ru to Q and/or hpp to Q
4.66	266	0.0364	H-16(β)→L(β) (13%) H-2(β)→L+5(β) (26%)	Ru to tpy; hpp to tpy; Q to tpy
4.67	265	0.0569	H-16(β)→LUMO(β) (15%) H-2(β)→L+5(β) (13%)	Q to tpy; hpp to tpy
4.70	264	0.0295	H-5(α)→L+3(α) (12%)	Ru to py; tpy to py; hpp to py
4.71	263	0.0868	H-2(β)→L+6(β) (10%)	Ru to tpy; hpp to tpy; Q to tpy
4.91	253	0.119	HOMO(β)→L+8(β) (15%)	Ru to tpy and/or hpp to tpy; Ru to py and/or hpp to py
4.96	250	0.0311	H-3(α)→L+4(α) (10%)	Ru to tpy; hpp to tpy
4.98	249	0.0291	H-2(α)→L+5(α) (12%) HOMO(β)→L+8(β) (14%)	Ru to tpy; Q to tpy; hpp to tpy
5.02	247	0.0455	H-9(β)→L+1(β) (12%)	Ru to tpy and/or hpp to tpy ; Ru to py and/or hpp to py
5.04	246	0.0339	H-5(α)→L+5(α) (14%) H-3(α)→L+5(α) (17%) H-1(α)→L+7(α) (23%)	Ru to py; hpp to py
5.11	242	0.0811	H-2(α)→L+6(α) (23%)	Ru to tpy; QpyG to tpy
5.13	242	0.0319	H-9(α)→L+2(α) (12%) HOMO(α)→L+7(α) (16%)	Ru to Q; hpp to Q
5.15	241	0.0557	H-3(β)→L+6(β) (11%) HOMO(β)→L+9(β) (18%)	py to hpp; Q to hpp

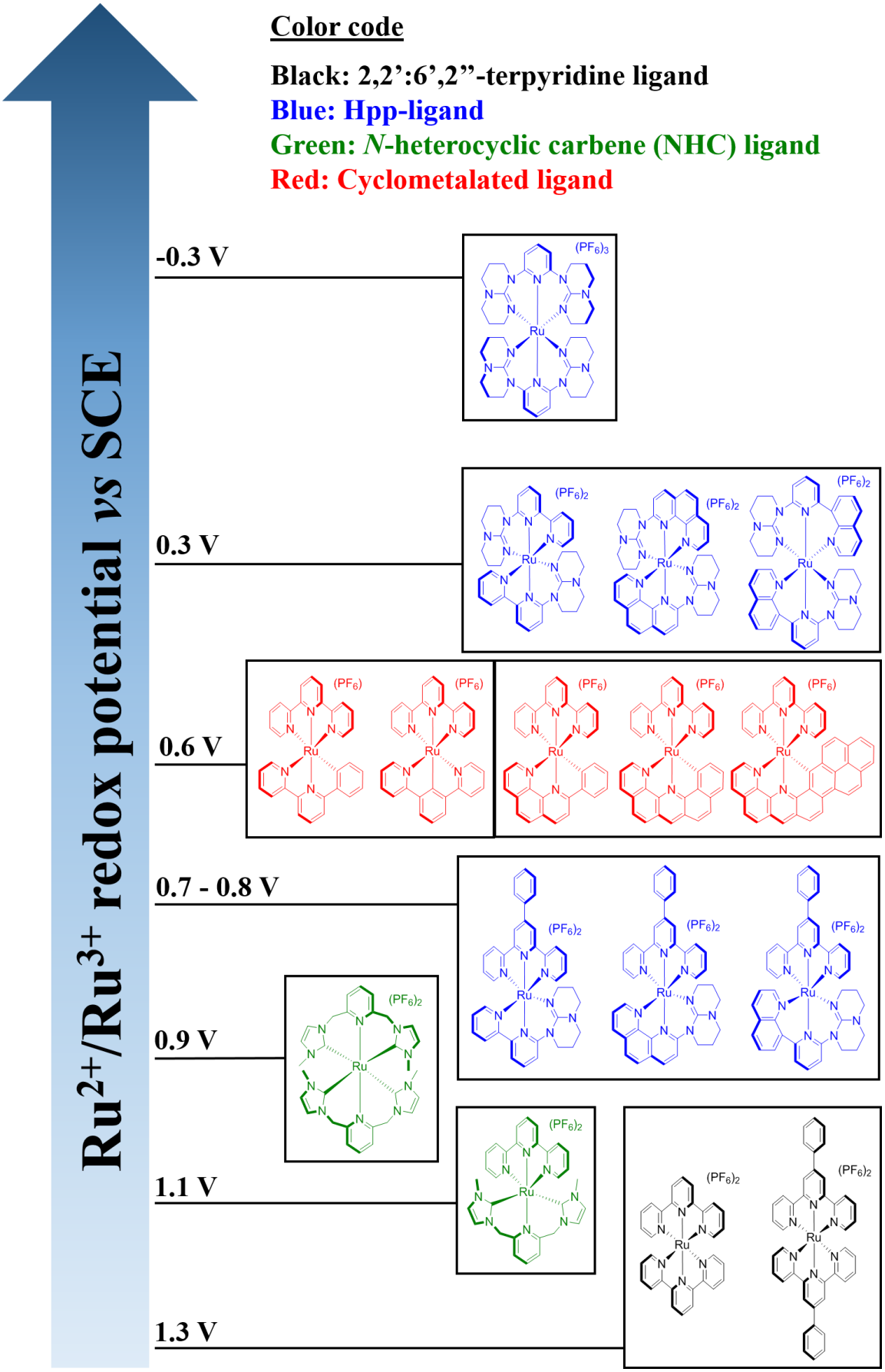

Figure S12 - Ru^{2+}/Ru^{3+} redox potentials comparison.

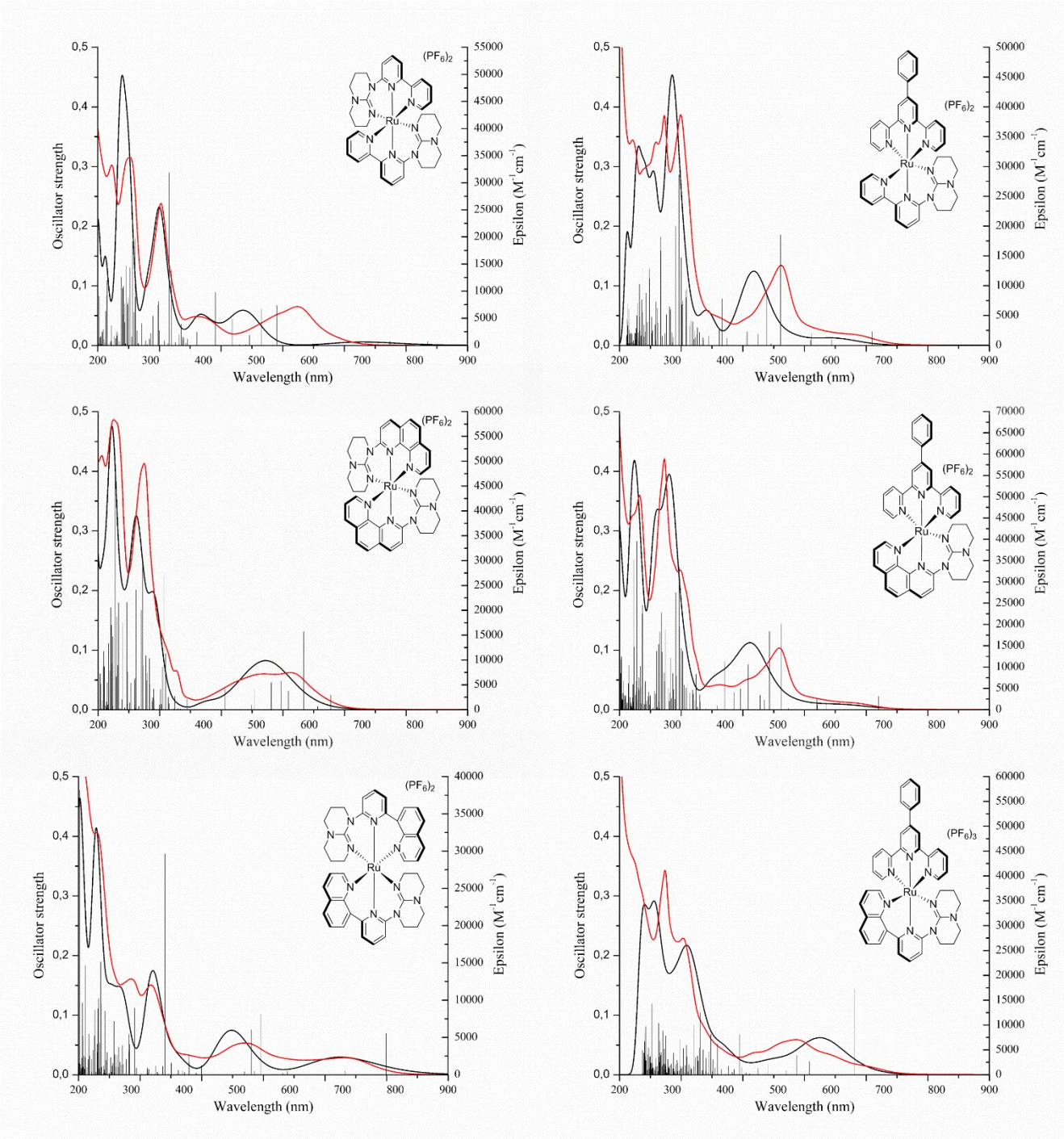

Figure S13 - Comparison of the experimental (red) absorption spectra recorded in acetonitrile and the TD-DFT (black) simulated (PBE0/LANL2DZ; CPCM: CH_3CN) absorption spectrum for the homoleptic complexes **4-6** (left) and heteroleptic complexes **7-9 (**right).

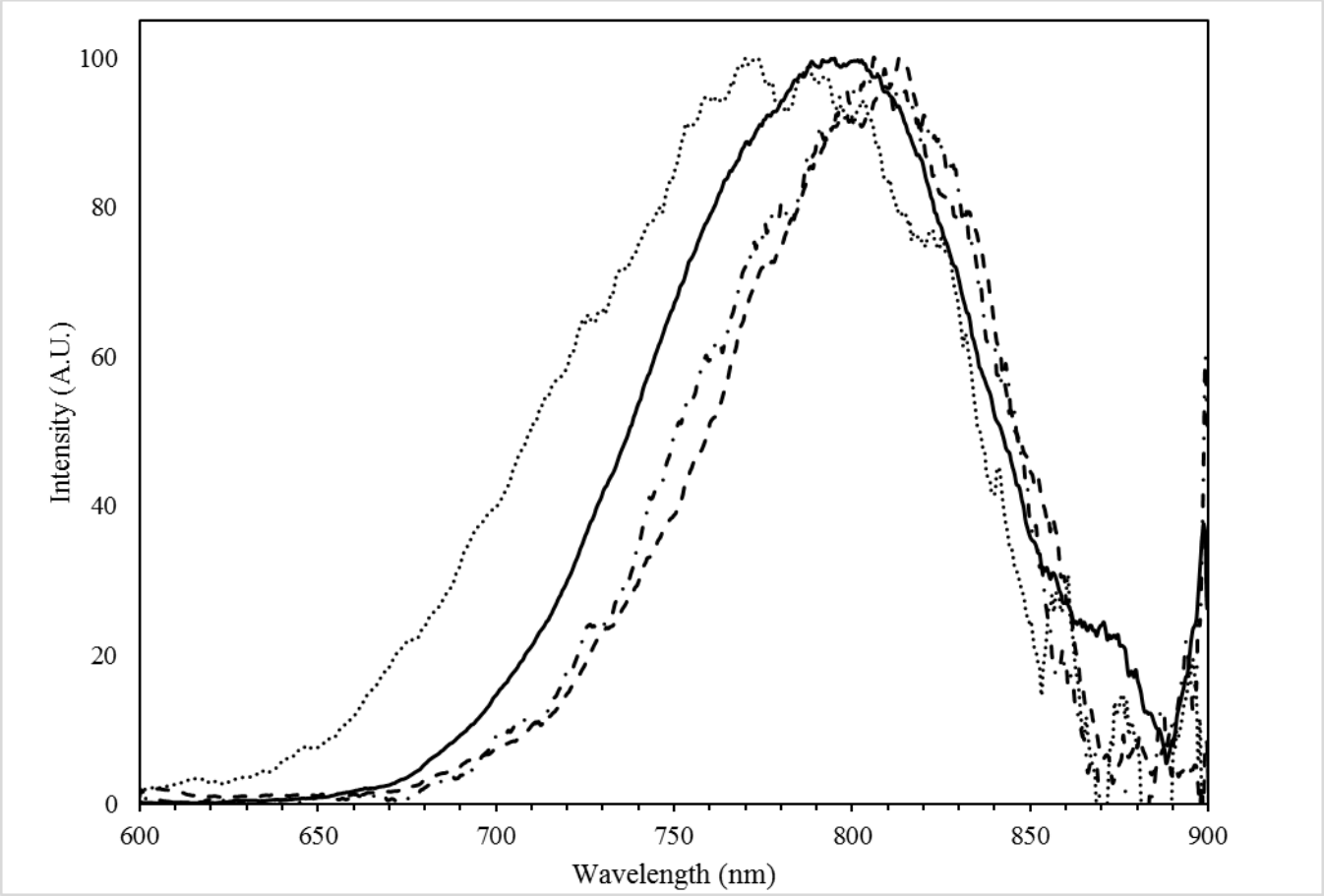

Figure S14 – Normalized luminescence spectra of the homoleptic complexes **4** (plain) and **5** (dots) as well as the heteroleptic complexes **7** (dash) and **8** (dash-dots) obtained in deaerated MeCN solution at ambient temperature.

4. References

[1] N. G. Connelly, W. E. Geiger, *Chem. Rev.* **1996**, *96*, 877-910.

[2] I. P. Evans, A. Spencer, G. Wilkinson, *J. Chem. Soc., Dalton Trans.* **1973**, 204-209.

[3] Y. Q. Fang, G. S. Hanan, *Synlett* **2003**, *6*, 852-854.

[4] F. Ferretti, E. Gallo, F. Ragaini, *J. Organomet. Chem.* **2014**, *771*, 59-67.

[5] D. J. Wasylenko, C. Ganesamoorthy, B. D. Koivisto, M. A. Henderson, C. P. Berlinguette, *Inorg. Chem.* **2010**, *49*, 2202-2209.